Stem Cell Reports
Article

OPEN ACCESS

Purification of GFRα1+ and GFRα1– Spermatogonial Stem Cells Reveals a Niche-Dependent Mechanism for Fate Determination

Alina Garbuzov,[1,3,6] Matthew F. Pech,[1,2,6] Kazuteru Hasegawa,[1] Meena Sukhwani,[4] Ruixuan J. Zhang,[1] Kyle E. Orwig,[4] and Steven E. Artandi[1,2,5,*]

[1]Department of Medicine, Stanford University School of Medicine, Stanford, CA 94305, USA
[2]Cancer Biology Program, Stanford University School of Medicine, Stanford, CA 94305, USA
[3]Department of Genetics, Stanford University, Stanford, CA 94305, USA
[4]Department of Obstetrics, Gynecology and Reproductive Sciences, University of Pittsburgh School of Medicine, Magee-Womens Research Institute, Pittsburgh, PA 15213, USA
[5]Department of Biochemistry, Stanford University School of Medicine, Stanford, CA 94305, USA
[6]Co-first author
*Correspondence: sartandi@stanford.edu
https://doi.org/10.1016/j.stemcr.2017.12.009

SUMMARY

Undifferentiated spermatogonia comprise a pool of stem cells and progenitor cells that show heterogeneous expression of markers, including the cell surface receptor GFRα1. Technical challenges in isolation of GFRα1+ versus GFRα1– undifferentiated spermatogonia have precluded the comparative molecular characterization of these subpopulations and their functional evaluation as stem cells. Here, we develop a method to purify these subpopulations by fluorescence-activated cell sorting and show that GFRα1+ and GFRα1– undifferentiated spermatogonia both demonstrate elevated transplantation activity, while differing principally in receptor tyrosine kinase signaling and cell cycle. We identify the cell surface molecule melanocyte cell adhesion molecule (MCAM) as differentially expressed in these populations and show that antibodies to MCAM allow isolation of highly enriched populations of GFRα1+ and GFRα1– spermatogonia from adult, wild-type mice. In germ cell culture, GFRα1– cells upregulate MCAM expression in response to glial cell line-derived neurotrophic factor (GDNF)/fibroblast growth factor (FGF) stimulation. In transplanted hosts, GFRα1– spermatogonia yield GFRα1+ spermatogonia and restore spermatogenesis, albeit at lower rates than their GFRα1+ counterparts. Together, these data provide support for a model of a stem cell pool in which the GFRα1+ and GFRα1– cells are closely related but show key cell-intrinsic differences and can interconvert between the two states based, in part, on access to niche factors.

INTRODUCTION

In tissues that require continuous renewal during life, stem cells fuel the generation of differentiated progeny. The ability to identify pathways important for stem cell function and to distinguish between populations with self-renewal capacity or commitment requires a robust method for isolating defined populations as well as a means for testing their stem cell potential via transplantation. In the mammalian testis, spermatogonial stem cells (SSCs) are the mitotic cells that maintain the germline by undergoing both self-renewal and differentiation, eventually yielding haploid sperm (Spradling et al., 2011). The exact identity and nature of the SSC pool remains incompletely understood.

SSCs, and all cells with transplantation potential in the testis, reside in a population of "undifferentiated type A" spermatogonia (A-undiff), named originally based on their undifferentiated morphology (Huckins, 1971). These rare cells on the basement membrane of seminiferous tubules are found as single cells, pairs, and chains of 4 to 16 cells (termed A_{single}, A_{pair}, and $A_{aligned4\text{-}16}$, respectively), as incomplete cell division in this compartment results in elongating cell syncytia. "Undifferentiated" spermatogonia mature to become "differentiated" spermatogonia, which are marked by expression of the cell surface receptor *Kit* (Schrans-Stassen et al., 1999). During each cycle of spermatogenesis, the vast majority of spermatogonia migrate luminally to enter meiosis. Based on histological observations, it was proposed that the SSC pool is comprised only of the A_{single} cells, and that division into A_{pair} represents commitment to a transiently amplifying progenitor (de Rooij, 1973; Huckins, 1971; Oakberg, 1971).

Recent studies have identified a number of genes that are expressed on a subset of A_{single} cells, including *Bmi1*, *Pax7*, and *Id4* (Aloisio et al., 2014; Helsel et al., 2017; Komai et al., 2014). In support of the A_{single} model, transplantation of ID4-GFP^{Bright} spermatogonia from juvenile testis achieved a high transplantation efficiency (Helsel et al., 2017). However, whether all ID4+ cells function as SSCs in the adult or whether ID4 marks the entire population of SSCs is unclear.

Short-chain undifferentiated spermatogonia tend to express GFRα1, the cell surface receptor for the key self-renewal factor glial cell line-derived neurotrophic factor (GDNF) (Meng et al., 2000). Lineage tracing using GFRα1– CreER knockin mice revealed that GFRα1+ cells can give rise to long-term labeling of the germ cell compartment, indicating that SSCs reside within the GFRα1+ population (Hara et al., 2014; Nakagawa et al., 2007). Only a subset of undifferentiated spermatogonia express GFRα1.

This is an open access article under the CC BY-NC-ND license (http://creativecommons.org/licenses/by-nc-nd/4.0/).

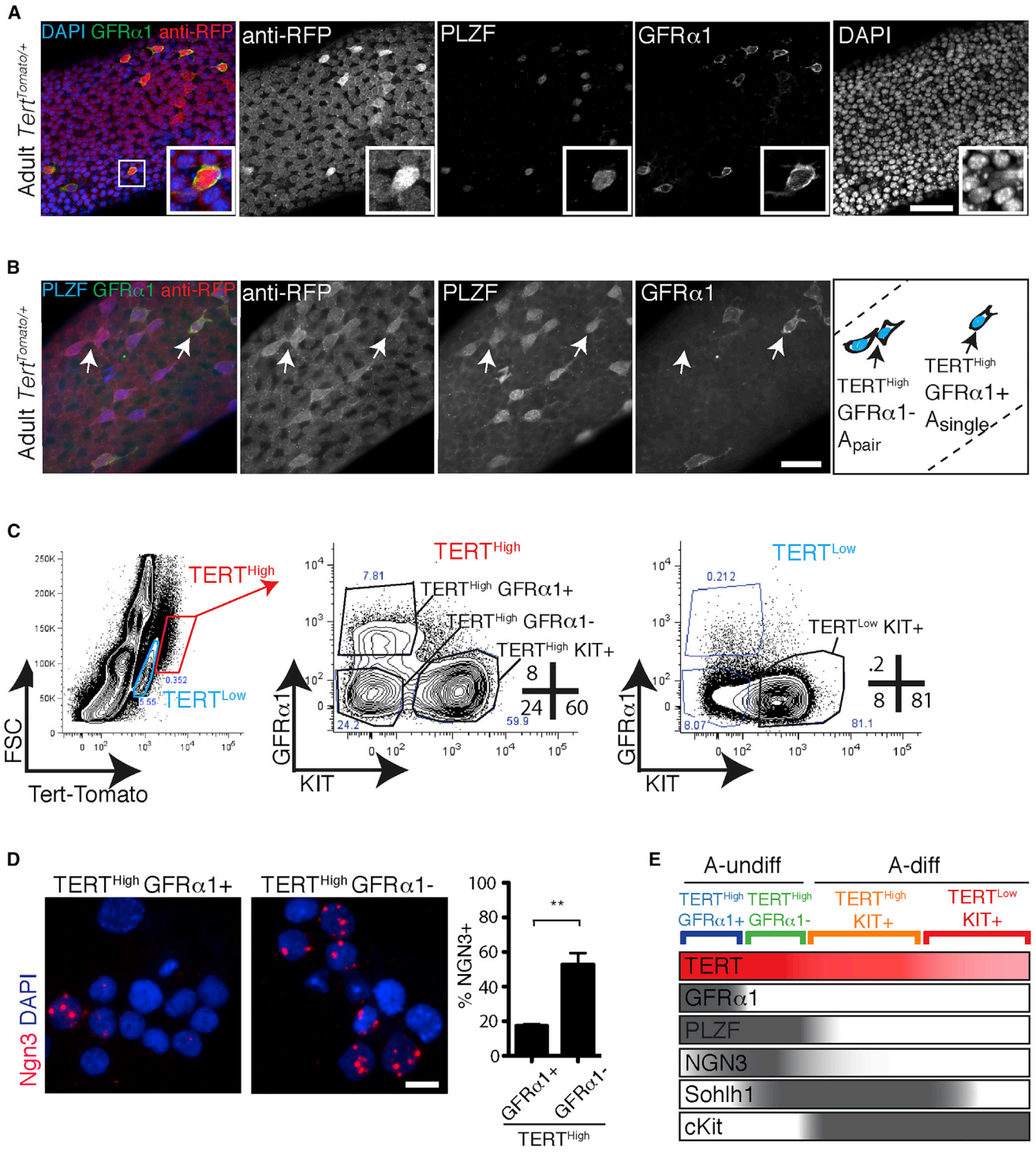

Figure 1. High Telomerase Expression Enables the Purification and Characterization of GFRα1+ and GFRα1– Undifferentiated Spermatogonia

(A) Whole-mount analysis of adult seminiferous tubules immunostained for GFRα1, PLZF, and anti-RFP in *Tert*$^{Tomato/+}$ seminiferous tubules. A total of 99.3% ± 0.5% of GFRα1+ PLZF+ cells were Tert-Tomato+ (N = 370 cells; N = 4 mice); 99.8% ± 0.1% GFRα1– PLZF+ cells were Tert-Tomato+ (N = 1900 cells; N = 6 mice). Scale bar, 50 μm.

(B) Whole-mount analysis of adult seminiferous tubules immunostained for GFRα1, PLZF, and anti-RFP in *Tert*$^{Tomato/+}$ seminiferous tubules. White arrows point to TERT^{High} GFRα1– A-paired (left arrow) and TERT^{High} GFRα1– A-single (right arrow) spermatogonia. Scale bar, 50 μm.

(legend continued on next page)

Seventy percent of undifferentiated spermatogonia do not express GFRα1, including 10%–30% of A_{single} and 25%–50% of A_{pair} (Gassei and Orwig, 2013; Grasso et al., 2012; Nakagawa et al., 2010), and the functional properties of these cell types are largely unexplored. The behavior of GFRα1– undifferentiated spermatogonia has been inferred by analyzing Neurogenin3-positive (NGN3+) cells, whose expression imperfectly marks the GFRα1– state. Analysis of NGN3-CreER knockin mice showed that NGN3+ cells can give rise to long-term labeling in a small subset of tracing events homeostatically, and to a greater degree after injury (Nakagawa et al., 2007, 2010). However, approximately 10% of NGN3+ cells are also GFRα1+, so whether self-renewal potential is found outside of the GFRα1+ compartment remains unknown. Alternative approaches are required to understand the properties of GFRα1– spermatogonia.

Transplantation is a rigorous assay for stem cell potential and has been used extensively to quantify functional SSCs (Brinster and Zimmermann, 1994). Previous work has revealed that the SSC pool may reside within spermatogonia expressing *Thy1*, *Itga6*, *Itgb1*, *Cdh1*, *Id4*, and *Pax7*, among others (Aloisio et al., 2014; Helsel et al., 2017; Kubota et al., 2003; Phillips et al., 2010; Shinohara et al., 1999; Tokuda et al., 2007). Although GFRα1– expressing spermatogonia are thought to be among the most primitive cells in the SSC differentiation hierarchy, attempts to transplant this population did not show enrichment for SSC-repopulating activity (Buageaw et al., 2005; Grisanti et al., 2009).

We previously discovered that PLZF+ undifferentiated spermatogonia are characterized by high levels of telomerase, the enzyme that synthesizes telomere DNA repeats at chromosome ends (Pech et al., 2015). By generating $Tert^{Tomato/+}$ reporter knockin mice, we identified a gradient of *Tert* transcription in the testis and used it to isolate undifferentiated spermatogonia. We also found that telomere dysfunction in $Tert^{-/-}$ mice induced depletion of the PLZF+ A-undiff pool over time, providing a cellular mechanism to explain the established infertility phenotype in telomerase knockout mouse strains (Lee et al., 1998; Pech et al., 2015). In this study, we develop methods to isolate highly purified populations of GFRα1–positive and GFRα1–negative undifferentiated spermatogonia from the testes of adult $Tert^{Tomato/+}$ reporter mice and from wild-type mice. We leverage these techniques to define transcriptome-wide features and functional differences between these two cell populations that define the SSC pool.

RESULTS

Purification of GFRα1+ and GFRα1– Undifferentiated Spermatogonia from Adult $Tert^{Tomato/+}$ Reporter Mice

Using a Tert-Tomato transcriptional reporter of telomerase activity, we previously showed that $TERT^{High}$ KIT– population represents a pure population of PLZF+ undifferentiated spermatogonia (Pech et al., 2015). To determine the relationship between telomerase expression and GFRα1 expression, we performed whole-mount microscopy on adult seminiferous tubules. Triple-staining for PLZF, GFRα1 and Tomato revealed that effectively all GFRα1+ cells express Tert-Tomato (99.3% ± 0.5%; Figure 1A). Tert-Tomato expression was similarly homogeneous (99.8% ± 0.1%) within GFRα1– PLZF+ undifferentiated spermatogonia, which included both long and short chains of cells (Figure 1B). Thus, both GFRα1+ and GFRα1– undifferentiated spermatogonia are characterized by high *Tert* promoter activity.

To develop a method for the isolation of GFRα1+ and GFRα1– undifferentiated spermatogonia using fluorescence-activated cell sorting (FACS), dissociated adult testes were stained with antibodies against GFRα1 and KIT. We previously found that the $TERT^{High}$ population comprised approximately 50% KIT– cells, representing undifferentiated spermatogonia, and 50% KIT+ cells, representing early differentiating spermatogonia. $TERT^{High}$ KIT– cells transplanted efficiently, whereas $TERT^{High}$ KIT+ cells failed to transplant (Pech et al., 2015). FACS of whole testes showed a subpopulation of $TERT^{High}$ KIT– cells were GFRα1+, and that the GFRα1+ cells represented approximately one-third of the $TERT^{High}$ KIT– population, consistent with whole-mount analysis. GFRα1+ cells were absent in all other populations, including $TERT^{Low}$ cells and $TERT^{High}$ KIT+ (Figure 1C). To further assess the identity of the purified $TERT^{High}$ KIT– GFRα1+ and GFRα1– populations, we isolated them by FACS and employed RNA *in situ* hybridization (ISH) to assay for NGN3 mRNA, whose expression has been used as a surrogate marker for GFRα1– spermatogonia. RNA ISH on sorted $TERT^{High}$ KIT– GFRα1+ and GFRα1– populations showed that 17% ± 1% of GFRα1+ cells express *Ngn3*, whereas 53% ± 7% of GFRα1– cells express *Ngn3*

(C) Flow cytometry measurement of GFRα1 and KIT expression in $TERT^{High}$ cells. Panels are representative of at least six independent FACS runs.

(D) *In situ* hybridization for NGN3 mRNA on FACS-sorted cells of the indicated immunophenotypes. Percentage of NGN3+ cells was quantified. Mean and SEM are shown. Scale bar, 25 μm. N = 5–6 mice; at least 2,000 cells counted per condition. **p = 0.012.

(E) Interpretation of identities of various sorted cell types, based on whole-mount, cytospin, immunophenotype, and neonatal time course data.

(p = 0.012, t test) (Figure 1D). These results indicate that *Ngn3* is differentially expressed between the TERT^{High} KIT– GFRα1+ and GFRα1– populations of undifferentiated spermatogonia, but that *Ngn3* expression alone is insufficient to discriminate the GFRα1+ and GFRα1– populations.

These results provide strong evidence for the successful isolation of GFRα1+ and GFRα1– undifferentiated spermatogonia, based on intrinsic *Tert* promoter strength and cell surface phenotypes (summary in Figure 1E). Employing the Tert-Tomato reporter was essential for successful purification of these populations. Sorting based on GFRα1 expression alone did not allow isolation of a pure population of GFRα1+ cells, nor did it allow the discrimination of GFRα1– undifferentiated spermatogonia due to background staining for GFRα1 in the meiotic cells and spermatids (Figure S1A). Enrichment for A-undiff cells using the *Tert* reporter allowed detection of distinct GFRα1+ and GFRα1– A-undiff populations, enabling subsequent molecular and functional studies.

Isolation and Transcriptional Profiling of Four Distinct Spermatogonial Populations

To identify the differences between the GFRα1+ and GFRα1– undifferentiated spermatogonia we performed RNA sequencing (RNA-seq) to identify the transcriptional features of each population. From four independent *Tert*$^{Tomato/+}$ mice, we sequenced the transcriptomes of FACS-purified TERT^{High} GFRα1+ KIT– cells and TERT^{High} GFRα1– KIT– cells. To put the transcriptional profiles in the context of spermatogenesis and differentiation, we also sequenced the population of TERT^{High} KIT+ cells and TERT^{Low} KIT+ cells (Pech et al., 2015), which represent early and late differentiating spermatogonia, respectively (Pech et al., 2015) (Figure S1). In addition, we isolated TERT^{High} Oct4-GFP double-positive spermatogonia from postnatal day 6 (P6) juveniles. Spermatogonia isolated from juvenile testes are enriched for stem cell activity and have previously been used to gain insights about adult SSCs (Helsel et al., 2017; Kanatsu-Shinohara et al., 2011).

By principal-component analysis (PCA) and unsupervised hierarchical clustering, biological replicates from the same populations clustered together, confirming our ability to isolate pure populations with discrete identities (Figures 2A and S2A). PCA showed three principal components that explain a large proportion of the variance between the populations. The four adult populations lined up along axis PC1 in an order that recapitulated differentiation: the TERT^{High} GFRα1+ KIT– cells and TERT^{High} GFRα1– KIT– populations were the leftmost populations, followed by TERT^{High} KIT+ cells further right, and with TERT^{Low} KIT+ cells as the rightmost population (Figure 2A). By PCA, the GFRα1+ and GFRα1– spermatogonia cluster together, and neither population is closer to the more differentiated TERT^{High} KIT+ cells. Our PCA analysis also showed that the P6 spermatogonia were significantly different from adult populations as they were separated from the rest of the samples along the PC2 axis (Figure 2A). We conclude that the PC1 axis captured the gene expression changes associated with differentiation, while the PC2 axis reflected changes associated with postnatal maturation. These data highlight the relatedness of the TERT^{High} GFRα1+ and TERT^{High} GFRα1– populations in the undifferentiated spermatogonia compartment.

GFRα1+ Spermatogonia Are Defined by a Transcriptional Signature of Active GDNF and Fibroblast Growth Factor Signaling

By differential expression analysis, we identified 578 significantly upregulated and 430 significantly downregulated genes in TERT^{High} GFRα1+ versus TERT^{High} GFRα1– cells (5% false discovery rate and 2-fold change cutoff; Figure 2B; Table S1). The GFRα1 receptor was one of the most differentially expressed genes, and its co-receptor Ret was also highly differentially expressed (16.9-fold change, $q = 3.9 \times 10^{-58}$; 2.7-fold, $q = 3.2 \times 10^{-5}$, respectively). Id4, a marker of A_{single} cells was also shown to be enriched in the GFRα1+ population (1.4-fold, $q = 4.5 \times 10^{-5}$). Furthermore, many of the most significantly upregulated genes in TERT^{High} GFRα1– cells were factors known to be enriched in long-chained A-undiff cells *Ngn3* (7.3-fold $q = 5.3 \times 10^{-16}$), *Nanos3* (2.8-fold, $q = 3.9 \times 10^{-7}$), *Sohlh1* (2.1-fold $q = 4.3 \times 10^{-4}$), *Sox3* (3.3-fold $q = 5.26 \times 10^{-5}$), and *Lin28a* (2.2-fold $q = 1.6 \times 10^{-10}$) (Chakraborty et al., 2014; Phillips et al., 2010; Suzuki et al., 2009, 2012) Thus, these transcriptomic studies have captured key markers of both GFRα1+ and GFRα1– undifferentiated spermatogonia.

GFRα1– GDNF signaling is required for both the *in vivo* maintenance of SSCs and their *ex vivo* culture (Kanatsu-Shinohara et al., 2003; Meng et al., 2000). Many genes originally identified as being GDNF responsive in germline stem cell culture systems (Oatley et al., 2006) were highly enriched in TERT^{High} GFRα1+ cells compared with TERT^{High} GFRα1– spermatogonia: *T* (57.3-fold, $q = 2.4 \times 10^{-10}$), *ETV5* (12.3-fold, $q = 3.4 \times 10^{-27}$), *EGR2* (19.8-fold, $q = 4.4 \times 10^{-99}$), *EGR3* (5.7-fold, $q = 4.7 \times 10^{-5}$), *BCL6B* (4.8-fold, $q = 4.5 \times 10^{-12}$), *Tspan8* (1.2-fold, $q = 7.3 \times 10^{-3}$), and *Lhx1* (15.5-fold, $q = 3.0 \times 10^{-11}$) (Figure 2B). In addition to GDNF, fibroblast growth factor (FGF) signaling is required for maintenance of SSCs *in vivo* and in culture (Hasegawa and Saga, 2014). Sprouty and Spred families of receptor tyrosine kinase (RTK) inhibitors and the DUSP family of MAPK phosphatases are transcriptionally induced during FGF responses (Branney et al., 2009), and this family of genes was highly upregulated in TERT^{High} GFRα1+ cells (Figure 2B). These findings provide evidence that TERT^{High} GFRα1+ cells actively receive FGF signals

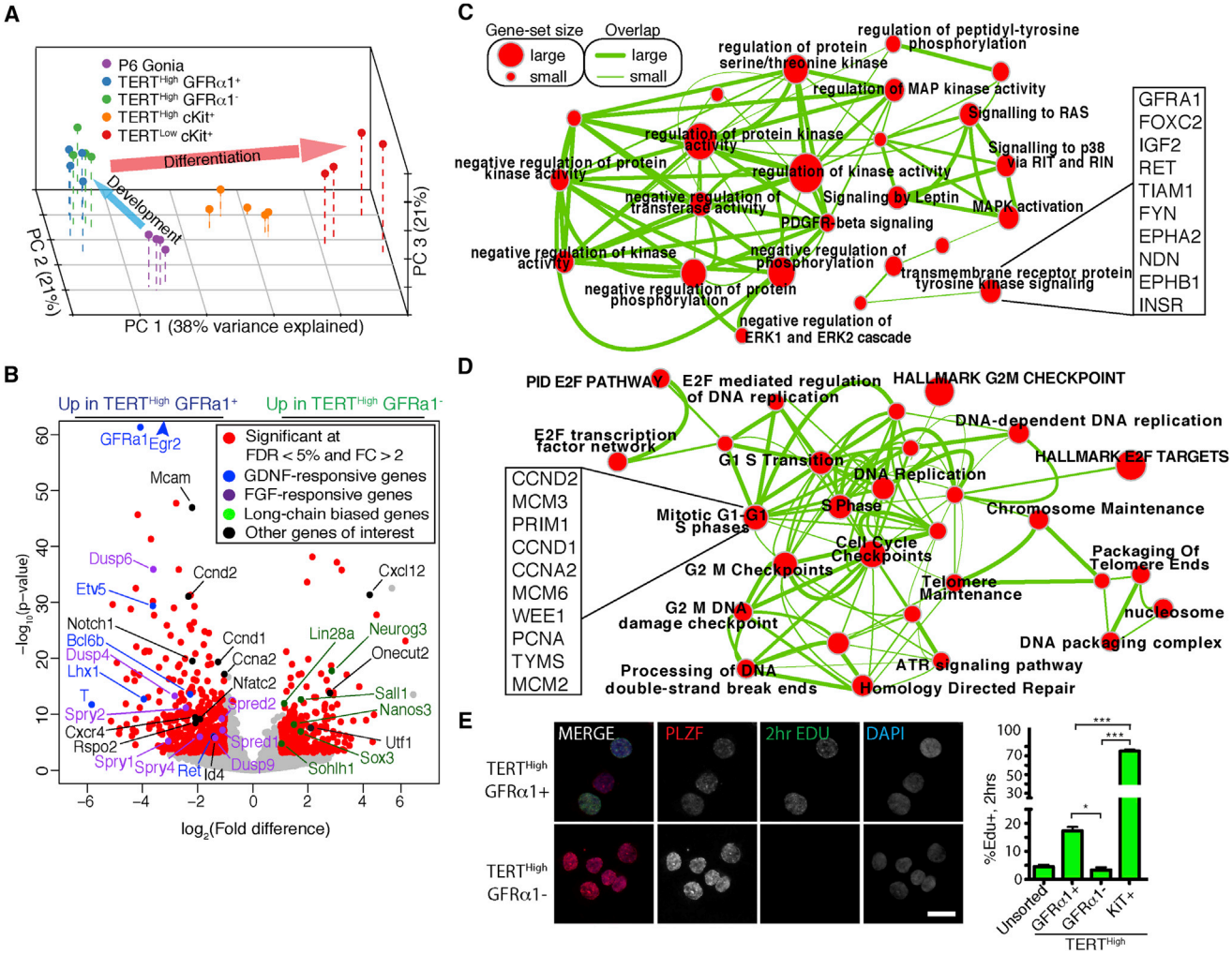

Figure 2. RNA-Seq Reveals That GFRα1+ Spermatogonia Are Defined by a Transcriptional Signature of Active GDNF and FGF Signaling

(A) Principal-component analysis (PCA) of transcriptomes from five isolated spermatogonial populations from adult and postnatal day 6 (P6) juvenile.

(B) Volcano plot of expression profiles comparing TERT^{High} GFRα1+ KIT− to TERT^{High} GFRα1− KIT− cells.

(C) MAP/ERK/protein phosphorylation cluster generated by Cytoscape Enrichment Map of gene set enrichment analysis (GSEA) results for TERT^{High} GFRα1+.

(D) Cell-cycle/proliferation cluster generated by Cytoscape Enrichment Map of GSEA results for TERT^{High} GFRα1+.

(E) Indicated cell types were sorted and cytospun. A 2 hr EdU pulse was visualized using Click chemistry, and the cells were then immunostained for the undifferentiated spermatogonia marker PLZF. Scale bar, 25 μm. Percentage of EdU+ cells was quantified. Mean and SEM are shown. (N = 5 mice; N = 900–10,000 cells per condition). *p < 0.05; ***p < 0.001.

in vivo. Taken together, these transcriptomic studies indicate a specific induction of GDNF- and FGF-regulated genes in GFRα1+ cells.

To understand the transcriptomes in these two populations more generally, we analyzed the differentially expressed genes by gene set enrichment analysis and visualized the results using Cytoscape Enrichment Map (Merico et al., 2010). Three major clusters of enriched functional gene sets were found in genes upregulated in GFRα1+ cells (p-value cutoff, 0.001). The first cluster involves RTK-RAS-MAPK signaling and protein phosphorylation (Figure 2C). The RAS-MAPK pathway is known to be important downstream of GDNF and FGF signaling (Hasegawa et al., 2013; He et al., 2008). Numerous gene sets related to RTK-RAS-MAPK signaling were associated with genes upregulated in GFRα1+ cells. Many core genes in this

enrichment cluster are the GDNF/FGF-responsive genes highlighted in the volcano plot (Figure 2B).

The second cluster involves cell-cycle progression, E2F transcription factor targets, DNA packaging, and replication (Figure 2D). These findings suggest a difference in cell-cycle activity between the GFRα1+ and GFRα1– undifferentiated spermatogonia. To test this idea, we assayed proliferation by *in vivo* 5-ethynyl-2′-deoxyuridine (EdU) labeling, followed by FACS purification, cytospin, and EdU detection. We found a marked difference in cell-cycle status between the two subpopulations of undifferentiated spermatogonia: GFRα1+ cells showed an S-phase fraction of 17.4% ± 1.4%, while GFRα1– cells exhibited an S-phase fractions of 3.3% ± 0.9% ($p = 0.033$, t test) (Figure 2E). These finding are consistent with the role for GDNF in spermatogonial self-renewal and proliferation (Meng et al., 2000; Tadokoro et al., 2002). The third, smaller cluster involved genes associated with morphogenesis and epithelium development (Figure S2B). Taken together, transcriptome and cell-cycle data suggest that GFRα1+ undifferentiated spermatogonia receive critical self-renewal and proliferation signals from their environment and that downregulating these pathways is an important characteristic of the transition to the GFRα1– state.

To understand the relationships between GFRα1+ and GFRα1– undifferentiated spermatogonia and other selections of undifferentiated spermatogonia, we compared the transcriptomes of GFRα1+ and GFRα1– cells with those of ID4-Bright cells, which show high transplantation potential, and ID4-Dim cells (Helsel et al., 2017). By differential expression analysis, the ID4-Bright and GFRa1+ undifferentiated spermatogonia were similar in expression of genes important for SSC maintenance and self-renewal, including: *GFRa1*, *Taf4b*, *Zbtb16*, *Bcl6b*, *Lhx1*, *T*, and *Pou3f1*, among others (Figure S3A). ID4 was enriched in ID4-Bright cells compared with GFRa1+ cells. Surprisingly, we found a number of genes associated with differentiated spermatogonia enriched in the ID4-Bright cells, including *Stra8*, *Alcam*, *Sycp1*, *Nanos3*, *Dmrt1*, *Sox3*, *Sohlh1*, and *Kit* (Figure S3A). A similar pattern was also seen in a comparison of GFRa1– cells with ID4-Bright cells (Figure S3B). PCA on the two ID4+ populations and our five populations to assess their relatedness revealed that both the ID4-Bright and the ID4-Dim cells cluster closely with the $TERT^{High}$ cells we isolated from day 6 neonates (P6) (Figure S3C). This relationship was also seen using unsupervised hierarchical clustering (Figure S3D). This similarity may occur because the ID4 populations in Helsel et al. were isolated from day 8 neonatal mice. Thus, the ID4-Bright cells from P8 mice are most similar transcriptionally to $TERT^{High}$ neonatal spermatogonia, and less similar to adult GFRα1+ and GFRα1– cells. These data highlight potential molecular differences between neonatal and adult SSC populations.

Elevated Melanocyte Cell Adhesion Molecule Is a Cell Surface Marker of the GFRα1+ State

Tert reporter mice enabled efficient purification of many spermatogonial subsets, but the lack of good antibodies specific for undifferentiated spermatogonial subpopulations currently makes it difficult to isolate these cells from wild-type mice. To identify new markers, we leveraged our transcriptome datasets from four distinct subpopulations of undifferentiated and differentiated spermatogonia. We used Short Time-series Expression Miner (STEM) (Ernst and Bar-Joseph, 2006) to compare gene expression simultaneously across all four populations. STEM analysis takes an ordered collection of expression datasets, assigns each gene to a profile bin and computationally identifies statistically enriched profiles. STEM analysis of $TERT^{High}$ GFRα1+ KIT– cells, $TERT^{High}$ GFRα1– KIT– cells, $TERT^{High}$ KIT+, and $TERT^{Low}$ KIT+ cells identified nine enriched profiles (Figure 3A). We were specifically interested in genes that followed the expression profile of GFRα1 (Figure 3A, green pattern). STEM identified GFRα1, ETV5, and melanocyte cell adhesion molecules (MCAMs) as having highly similar expression profiles (Figure 3B and Table S2). MCAM, an immunoglobulin-superfamily surface protein shown to enrich for transplantation activity (Kanatsu-Shinohara et al., 2012), was also one of the top ten most differentially expressed genes between GFRα1+ and GFRα1– cells (Figure 2B; 4.6-fold change, $q = 4.4 \times 10^{-44}$). Thus, MCAM represents a candidate cell surface marker with an expression pattern similar to GFRα1. To test similarity at the protein level, we investigated MCAM expression using whole-mount immunostaining. MCAM protein was enriched in a subset of PLZF+ undifferentiated spermatogonia (Figure 3C). Elevated MCAM expression was restricted to short-chain PLZF+ cells. Co-staining revealed that these $MCAM^{High}$ cells were exclusively GFRα1+ PLZF+ spermatogonia (Figure 3C). Therefore, our analysis enabled the discovery of an independent marker, MCAM, for the GFRα1+ subset of undifferentiated spermatogonia.

Isolation of Both GFRα1+ and GFRα1– Undifferentiated Spermatogonia Based on Differential MCAM Expression Using FACS

As MCAM is expressed on the cell surface, we tested its ability to enrich for spermatogonial populations using FACS. Staining dissociated tubules for GFRα1 and MCAM revealed a population of double-positive GFRα1+ MCAM+ cells in the $TERT^{High}$ KIT– fraction. This double-positive population was not present in the $TERT^{Low}$ KIT+ fraction (Figure 3D). These GFRα1+ MCAM+ cells isolated by FACS correspond to the same population seen in whole-mount immunostaining (Figure 3C).

These results suggested that MCAM can be used to isolate GFRα1+ cells without relying on the Tert-Tomato reporter

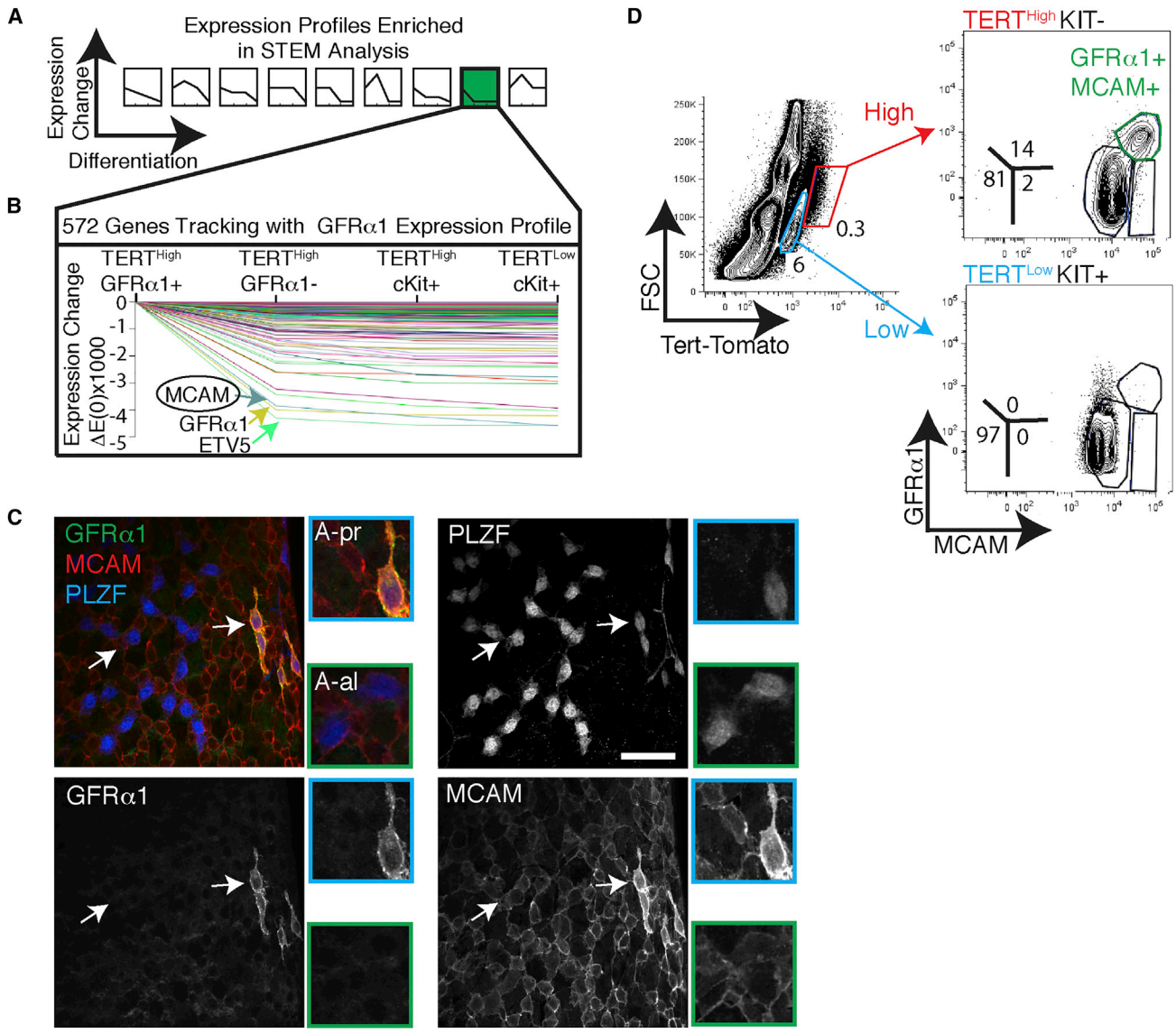

Figure 3. MCAM Is a Cell Surface Marker of the GFRα1+ State

(A) Nine patterns of gene expression changes across adult spermatogonial populations identified as statistically significant by Short Time-series Expression Miner (STEM).

(B) Details on STEM pattern no. 8, containing genes with peak expression in TERT^{High} GFRα1+ cells, with diminished expression in all other cell types. Genes of interest are highlighted. The entire list of 575 genes is found in Table S2.

(C) Whole-mount analysis of tubules triple-stained for MCAM, GFRα1, and PLZF. All 76/76 GFRα1+ cells were MCAM^{High}. White arrows point to cells shown in greater magnification in the panels to the right. Scale bar, 50 μm. N = 3 mice.

(D) Flow cytometry measurement of GFRα1 and MCAM expression in TERT^{High} KIT– cells and TERT^{Low} KIT+. Panels are representative of at least six independent FACS runs.

mouse or on GFRα1 staining. To test this hypothesis, we stained dissociated tubules from wild-type mice using antibodies against MCAM and KIT. By flow cytometry, the MCAM signal was sufficiently strong to separate three distinct populations by MCAM expression level: MCAM^{High}, MCAM^{Med}, and MCAM^{Low} (Figure 4A). The MCAM^{High} population was highly enriched for KIT– cells (85%–90% KIT–) (Figure S4A). The MCAM^{Med} and MCAM^{Low} populations were predominantly KIT+ cells (Figures S4B and S4C). To determine if MCAM levels along with staining for KIT allow us to isolate GFRα1+ and GFRα1– undifferentiated spermatogonia, we sorted MCAM^{High}

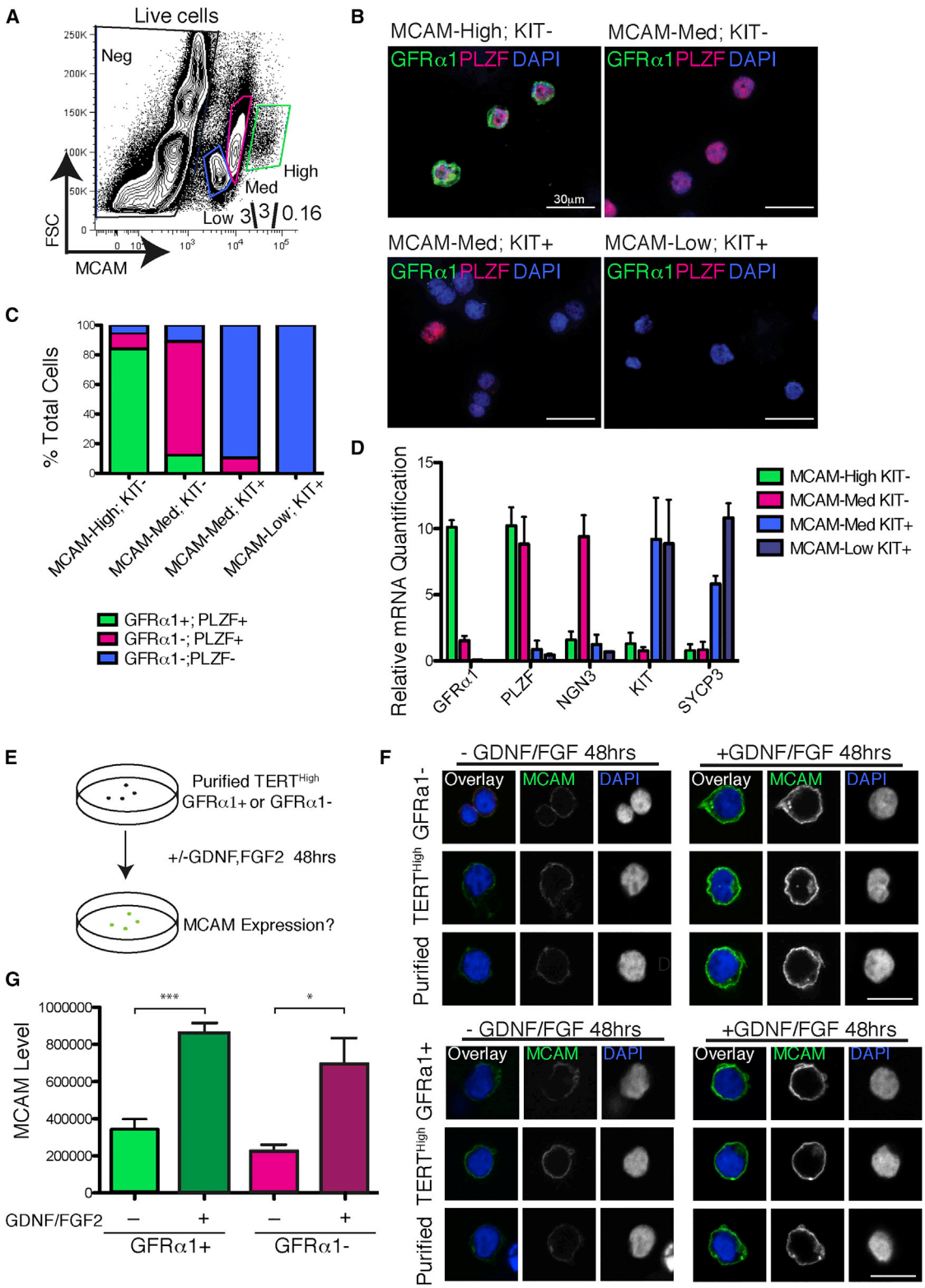

(legend on next page)

KIT– cells, MCAM^{Med} KIT– cells, MCAM^{Med} KIT+ cells, and MCAM^{Low} KIT+ cells, cytospun them, and stained them for GFRα1 and PLZF (Figure 4B). The MCAM^{High} KIT– cells were 84% GFRα1+ PLZF+. The MCAM^{Med} KIT– population was 77% GFRα1– PLZF+. The MCAM^{Med} KIT+ population was 90% GFRα1– PLZF–. And the MCAM^{Low} KIT+ population was 100% GFRα1– PLZF– (Figure 4C). Therefore, this approach allows the isolation of highly enriched populations of A-undiff GFRα1+ spermatogonia as MCAM^{High} KIT– and A-undiff GFRα1– spermatogonia as MCAM^{Med} KIT–.

To validate our data, we performed qRT-PCR for a variety of marks of undifferentiated and differentiated spermatogonia. By qPCR, MCAM^{High} KIT+ cells expressed high levels of GFRα1 and PLZF mRNA. MCAM^{Med} KIT– cells expressed 10-fold less GFRα1 mRNA than MCAM^{High} KIT+ and high levels of PLZF and NGN3. MCAM^{Med} KIT+ cells and MCAM^{Low} KIT+ expressed high levels of KIT and SYCP3 mRNA (Figure 4D). Our findings provide a robust protocol for isolation of phenotypically defined subtypes of undifferentiated spermatogonia from adult wild-type mice. MCAM provides a marked advantage over GFRα1 staining due to an improved signal-to-noise ratio with this combination of antigen and antibody.

Our RNA-seq analysis suggests that the main difference between GFRα1+ and GFRα1– undifferentiated spermatogonia is active GDNF/FGF signaling. We wondered if MCAM were a GDNF/FGF-responsive gene. To test this hypothesis, we used FACS to isolate pure populations of GFRα1+ and GFRα1– cells and then cultured them in germline stem cell medium either with or without GDNF/FGF (Figure 4E) (Kanatsu-Shinohara et al., 2003). The high level of MCAM expression in freshly isolated SSCs was indeed dependent on exposure to GDNF/FGF: *ex vivo* culture of TERT^{High} GFRα1+ cells in the absence of these cytokines led to a rapid downregulation of surface MCAM levels. Similarly, TERT^{High} GFRα1– cells exposed to GDNF/FGF had higher MCAM levels than TERT^{High} GFRα1– cells cultured in the absence of these cytokines (Figure 4F). Quantifying the changes in MCAM antibody staining showed a significant induction of MCAM expression with GDNF/FGF exposure (Figure 4G). Thus, both GFRα1+ and GFRα1– retain the ability to respond in culture to GDNF/FGF, leading to robust induction of MCAM. Taken together, GFRα1+ and GFRα1– undifferentiated spermatogonia are efficiently isolated on the basis of surface MCAM expression, and elevated MCAM protein in GFRα1+ cells likely reflects active GDNF/FGF signaling in this compartment.

Elevated Stem Cell Repopulating Activity in Both GFRα1+ and GFRα1– Undifferentiated Spermatogonia

Based on the similarities between the GFRα1+ and GFRα1– cells, we hypothesized that the self-renewal capacity of GFRα1– cells may be revealed upon transplantation into an empty niche and we leveraged our ability to isolate both GFRα1+ and GFRα1– cells to compare their relative transplantation potential side-by-side. FACS-purified cells were assayed in terms of their ability to colonize the tubules of *Kit*$^{W/Wv}$ mice, which lack SSCs (Brinster and Zimmermann, 1994). Donor cells were permanently marked by breeding *Tert*$^{Tomato/+}$ mice to mouse strains with ubiquitous expression of either EGFP or β-galactosidase. FACS-sorted TERT^{High} GFRα1+ and TERT^{High} GFRα1– cells from adult donors were injected separately into the seminiferous tubules of *Kit*$^{W/Wv}$ recipients via the efferent bundle (Figure 5A). Stem cell frequency in bulk germ cells was assessed by transplanting FACS-sorted live cells that were not fractionated by antigen expression (unfractionated). Two months later, the total number of colonies was counted (Figure 5B).

TERT^{High} GFRα1+ cells transplanted at high efficiencies, achieving 65-fold enrichment for stem cell activity over unfractionated germ cells (72.5 ± 37 colonies per 100,000 cells; $p < 0.0001$ U test). TERT^{High} GFRα1– cells also showed robust transplantation, albeit at lower frequencies than TERT^{High} GFRα1+ cells ($p < 0.0005$ U test; GFRα1+ versus GFRα1–). TERT^{High} GFRα1– cells showed 25-fold enrichment in stem cell transplantation compared with unfractionated germ cells (28 ± 22 colonies per 100,000 cells; $p = 0.0189$ U test) (Figure 5C). Histological analysis confirmed that both types of A-undiff spermatogonia

Figure 4. MCAM Levels Can be Used to Isolate Both GFRα1+ and GFRα1– Undifferentiated Spermatogonia and Are Responsive to GDNF/FGF

(A) Flow cytometry measurement of MCAM levels in whole adult testis from wild-type mice.

(B) Indicated populations were sorted from wild-type mice, cytopun, and stained for GFRα1, PLZF, and DAPI.

(C) Quantification of (B) showing fraction of GFRα1+ PLZF+, GFRα1– PLZF+, and GFRα1– PLZF– cells in each MCAM population. N = 3 mice pooled; N = 1,524 cells.

(D) qRT-PCR for indicated SSC and differentiation markers from cells sorted based on MCAM expression and KIT. Mean and SEM are shown.

(E) Experimental outline of cell culture experiments. Indicated cells populations were sorted and cultured in basal GS medium supplemented with or without 50 ng/mL GDNF and 20 ng/mL FGF2. Forty-eight hours later, anti-MCAM immunofluorescence was performed.

(F) Effect of GDNF/FGF on MCAM expression. TERT^{High} GFRα1+ cells and TERT^{High} GFRα1– cells were stained for MCAM and DAPI after 48 hr of culture. Scale bar, 15 μm.

(G) Quantification of (E). (N = 4 mice; N = 50 cells). Mean and SEM are shown. *$p < 0.05$; ***$p < 0.001$.

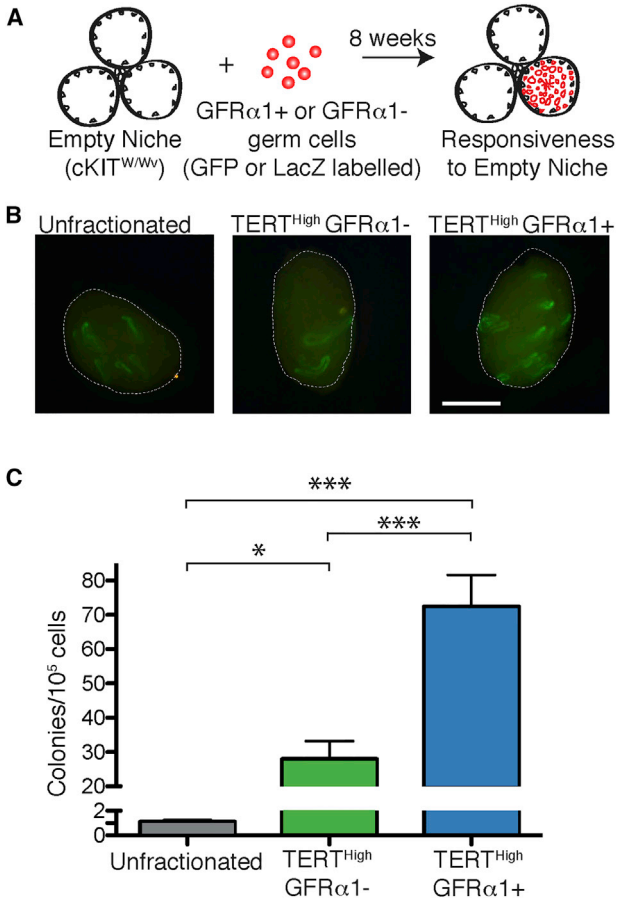

Figure 5. Elevated Stem Cell Repopulating Activity in GFRα1+ and GFRα1– Undifferentiated Spermatogonia

(A) Experimental outline of transplant experiments. Tert-Tomato cells permanently labeled by ubiquitous GFP or LacZ expression were transplanted into sterile *Kit*$^{W/Wv}$ recipients. Colonies were counted 2 months post-injection.

(B) Representative EGFP epifluorescence in recipient *Kit*$^{W/Wv}$ mice 8 weeks after transplantation of cells shown in (A). White lines represent boundary of the testis. "Unfractionated" represents the transplantation of FACS-sorted live cells not fractionated by Tert-Tomato expression or immunophenotype. Scale bar, 2 μm.

(C) Quantification of transplant results shown in (B). Colony counts were normalized to 10^5 cells. Mean and SEM are shown. p Values are from two-tailed Mann-Whitney test. N = 16–18 recipient testes per condition. *p = 0.019 ***p < 0.0005.

were capable of full reconstitution of spermatogenesis post-transplant (Figure S5B). Importantly, stringent sorting conditions led to very high purity of donor cell preparations, as confirmed by re-analysis of the sorted cells prior to transplant (Figure S5A). Thus, we find that GFRα1+ cells show high transplantation efficiency, but that GFRα1– cells also retain significant transplantation potential. Given that the pool of GFRα1– undifferentiated spermatogonia is three times as large as the GFRα1+ pool, the *total* number of GFRα1– stem cells is comparable with the total number of GFRα1+ stem cells in the testis.

GFRα1– A-Undiff Cells Regenerate the GFRα1+ State after Transplantation

The considerable stem cell potential in GFRα1– spermatogonia prompted us to explore the features of GFRα1– stem cell self-renewal. To address whether spermatogenesis from GFRα1– cells entailed the regeneration of GFRα1+ cells, whole-mount analysis of GFRα1 expression was performed on recipient testes 2 months post-transplantation of TERT^{High} GFRα1– cells (Figure 6A). These GFRα1– cells robustly gave rise to colonies containing TERT^{High} GFRα1+ cells (Figure 6B). The colonies also contained TERT^{High} MCAM^{High} cells (Figure 6C). Our data show the ability, *in vivo*, of GFRα1– cells to respond to niche signals and convert to the GFRα1+ state. These data highlight the functional similarity between the GFRα1+ and the GFRα1– undifferentiated spermatogonia as revealed by the transplantation assay.

DISCUSSION

A Heterogeneous Adult Germline Stem Cell Pool: GFRα1+ and GFRα1– Undifferentiated Spermatogonia Are Closely Related

We leveraged differences in *Tert* promoter strength, together with cell surface marker expression, to isolate pure populations of phenotypically defined spermatogonia subsets from adult testis. Our approach enables the isolation of both GFRα1+ and GFRα1– undifferentiated spermatogonia for functional and molecular analysis. These two populations of A-undiff cells show overall relatedness with key differences in signaling pathways. Both populations showed elevated frequencies of transplantation compared with unfractionated spermatogonia, with GFRα1+ cells transplanting approximately 2.6-fold more efficiently than GFRα1– cells. Most data have converged on the idea that SSCs are restricted to the short-chain population of A-undiff cells. Consistent with this idea, short-chain A-undiff cells are present throughout the spermatogenic cycle, whereas longer-chain A-undiff cells are ultimately depleted from the population through differentiation. Our data show that SSCs are highly enriched in the GFRα1+ fraction. These results are consistent with those of other laboratories using reporter mice for GFRα1+ and other markers within this short-chain population, including ID4, BMI1, and PAX7 (Aloisio et al., 2014; Helsel et al., 2017; Komai et al., 2014). It has been argued that these latter markers of subpopulations of short-chain A-undiff cells represent the true stem cells, but direct molecular

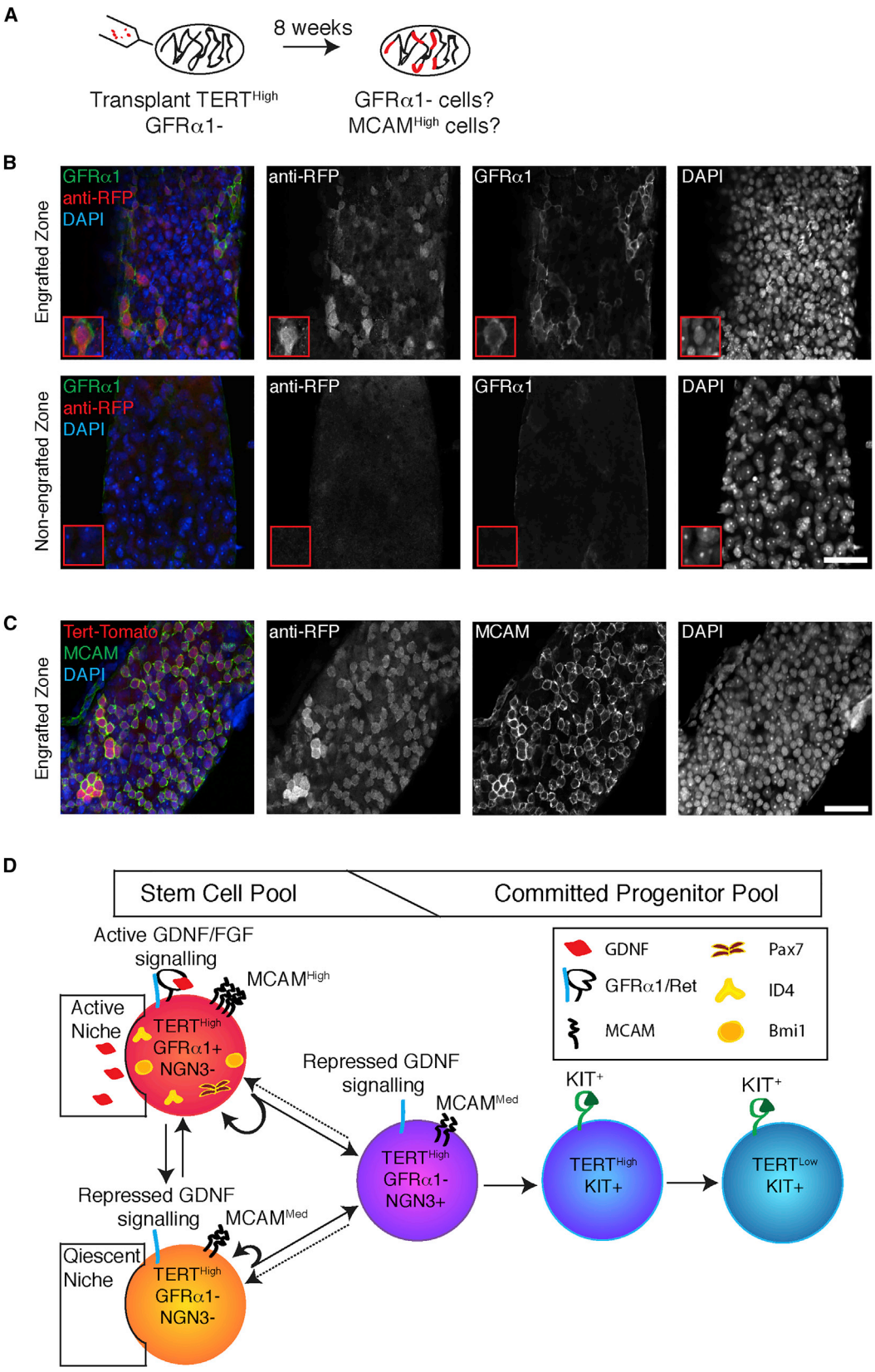

(legend on next page)

and functional comparisons of GFRα1+ cells bearing ID4, BMI1, or PAX7, with their GFRα1+ counterparts without expression of ID4, BMI1, or PAX7, have been lacking. Such direct comparisons will be required to understand functional heterogeneity within the GFRα1+ population. Our studies enabling the isolation of GFRα1+ cells using either GFRα1+ antibodies in conjunction with *Tert*$^{Tomato/+}$ mice, or MCAM antibodies in wild-type mice, may allow these ideas to be tested directly. In addition, approximately 20% of short-chain A-undiff cells are GFRα1– in steady state, and these cells have not been isolated or characterized for stem cell activity.

Our findings indicate that GFRα1– cells exhibit a surprising capacity for transplantation. SSCs in this fraction may reside in the short-chain GFRα1– fraction or in the elongating chains of PLZF+ A-undiff cells, or both these populations. If residing within the short-chain GFRα1– fraction, these cells may be in equilibrium with GFRα1+ cells, or may have unique characteristics that have not yet been revealed. If the SSCs defined here in the GFRα1– fraction reside in the elongating A-undiff population, the residual stem cell activity may reflect that some or many of these cells have not yet committed to differentiate. Our results showing elevated SSC activity in the TERT^{High} GFRα1– fraction suggests that many cells in this population have not yet fully committed. The ability of these cells to successfully transplant is also consistent with the likelihood that many GFRα1– cells are fated to differentiate to A-aligned spermatogonia during the spermatogenic cycle, as transplantation tests the ability of cells to function as stem cells. These distinctions are important to define the cellular and molecular mechanisms of self-renewal in the mammalian testis. We note that although the transplantation activity was 2.6 times lower in GFRα1– undifferentiated spermatogonia compared with GFRa1+ undifferentiated spermatogonia, GFRα1– cells are more abundant than their GFRα1+ counterparts, making the total number of potential stem cells comparable in each population. These data provide support for a model in which the GFRα1+ and GFRα1– cells together comprise a stem cell pool, and that some GFRα1– cells can convert to the GFRα1+ state based on exposure to niche factors (Figure 6D).

Transcriptional Similarity, but Distinct Regulation, of GDNF and FGF Signaling in GFRα1+ and GFRα1– Spermatogonia

Transcriptional analysis of GFRα1+ and GFRα1– undifferentiated spermatogonia revealed a previously unknown similarity between the two populations, in particular when compared with transcriptomes of neonatal spermatogonia, TERT^{High} KIT+ or TERT^{Low} KIT+ spermatogonia, which each cluster separately based on PCA and unsupervised hierarchical clustering. The differentially expressed genes between GFRα1+ and GFRα1– undifferentiated spermatogonia were enriched for gene sets including cell-cycle regulation and Ras/MEK/ERK signaling downstream of GFRα1/Ret binding of GDNF. Cyclin D1, D2, and A2 were in the top of differentially expressed genes between GFRα1+ and GFRα1– cells (Figures 2B and 2D; Table S1). As cyclin D2 has been shown to be important for GS cell self-renewal and long-term culture (Lee et al., 2009), and is expressed in type A spermatogonia *in vivo* (Beumer et al., 2000), we speculate that cell-cycle regulation is key for the SSC population *in vivo*. Differences in the abundance of each population during the seminiferous cycle may also contribute to the differences in S-phase fraction measured here, as NGN3+ cells are more abundant in stages IV-VII, at which time they are not proliferating (Ikami et al., 2015).

We found that ID4-Bright cells clustered most closely with our TERT^{High} neonatal spermatogonia, likely reflecting the neonatal origin of the ID4-Bright cells used for RNA-seq studies (Helsel et al., 2017). Although the neonatal ID4-Bright cells share expression of many stem cell genes with the adult GFRα1+ population, their overall transcriptomes are sufficiently different that they are most similar to other neonatal populations. These transcriptional differences may relate to expression of both SSC genes and differentiation genes within the ID4+ population. This combination of features reflects the peculiarities of the first, synchronized wave of spermatogenesis, which is faster than the adult cycle and features gonocytes that directly give rise to A_2 spermatogonia (Kluin et al., 1982; van Haaster and de Rooij, 1993). The extensive RNA-seq analysis performed here highlights key differences between neonatal and adult populations of spermatogonia.

Figure 6. *In Vivo* Conversion of GFRα1– Undifferentiated Spermatogonia to GFRα1+ Undifferentiated Spermatogonia

(A) Experimental outline of transplant experiments. GFRα1– Tert-Tomato cells permanently labeled by ubiquitous GFP or LacZ expression were transplanted into sterile *Kit*$^{W/Wv}$ recipients. Tubules were stained for MCAM and GFRα1 2 months post transplant.

(B) GFRα1 expression in colonies arising from transplanted TERT^{High} GFRα1– cells. Tert-Tomato used as a marker for the donor cells. Staining results are compared with regions of testis that were not colonized. Scale bar, 50 μm.

(C) MCAM expression in colonies arising from transplanted TERT^{High} GFRα1– cells. Tert-Tomato used as a marker for the donor cells. Scale bar, 50 μm.

(D) Model for a flexible hierarchy of adult spermatogonia. Cell surface features of different spermatogonial subtypes are highlighted. GFRα1– spermatogonia represent a poised state, competent to either differentiate or convert to GFRα1+ spermatogonia in a context-dependent fashion.

GFRα1– Spermatogonia Are Capable of Responding to GDNF/FGF Niche Signals in Culture

We found that, in culture, GFRα1– cells can respond to GDNF/FGF2 to upregulate MCAM to the levels of GFRα1+ cells. Consistent with this observation, we observed that GFRα1– cells and GFRα1+ cells share a requirement for GDNF and FGF for even short-term culture. The mechanism by which GFRα1– cells can sense GDNF/FGF is unclear, but may be due to low level receptor expression. Our molecular profiling showed a gradient of GFRα1 expression, similar to the gradient of MCAM expression (Figure 3B). Although GFRα1 mRNA is reduced by 16-fold in GFRα1– A-undiff cells compared with GFRα1+ cells (Table S1), GFRα1 mRNA remains 2.3-fold elevated in GFRα1– cells compared with $TERT^{High}$ KIT+ early differentiating spermatogonia ($q = 1.39 \times 10^{-17}$; Tables S2 and S3). Furthermore, FGFR1 and FGFR3 are both expressed on GFRα1+ and GFRα1– spermatogonia, and FGFR1 significantly decreases in $TERT^{High}$ KIT+ cells compared with GFRα1– cells (Table S3). Taken together, these results suggest that at least a subpopulation of GFRα1– cells retains the ability to respond to GDNF and FGF niche factors.

Isolation of Phenotypically Defined Spermatogonial Subpopulations from Adult Wild-Type Mice

Our purification of adult spermatogonia populations, together with RNA-seq, allowed us to identify MCAM as a useful cell surface marker enabling efficient purification of GFRα1+ and GFRα1– spermatogonial subtypes from adult wild-type mice. MCAM expression on spermatogonia was discovered by Kanatsu-Shinohara et al. (2012) in GS cell cultures. *In vivo*, MCAM expression was found on both undifferentiated and differentiating spermatogonia and CD9+ $EPCAM^{low}$ MCAM+ KIT– cells were enriched for SSC activity by transplantation (Kanatsu-Shinohara et al., 2012). Subsequently, sorting for MCAM+ KIT– was used to isolate Bmi1+ undifferentiated spermatogonia (Komai et al., 2014). Our results are consistent with MCAM enriching for SSCs; however, we revealed a clear gradient of MCAM surface expression that, when coupled with KIT expression, allows isolation of nearly pure populations of GFRa1+ and GFRa1– undifferentiated spermatogonia. The ability to isolate these cells from adult wild-type mice will facilitate the study of these populations and allow for future work to define additional molecular and functional features of these cell types in steady-state spermatogenesis.

EXPERIMENTAL PROCEDURES

Animals

$Tert^{Tomato/+}$ mice were described previously (Pech et al., 2015); $Kit^{W/Wv}$ mice were purchased (Jackson Laboratory, stock no. 100410). Experiments on adult mice were performed on males between 6 weeks and 3 months of age. All mice were treated in accordance with Association for Assessment and Accreditation of Laboratory Animal Care-approved guidelines at Stanford University.

Antibodies

The following antibodies were used for immunostaining and/or flow cytometry: MCAM-AF488 and MCAM-APC (Biolegend ME-9F1; rat monoclonal), Thy1.2-APC-Cy7 (Biolegend 3OH-12; rat monoclonal), SOHLH1 (gift of A. Rajkovic; rabbit polyclonal). Other antibodies used have been described previously (Pech et al., 2015)

Testes Dissociation and FACS Analysis

Testes were dissociated and FACS analyzed as previously described (Pech et al., 2015). For GFRα1 FACS staining, a biotinylated primary antibody was used, together with a secondary streptavidin-APC secondary (Jackson Immunoresearch) for 30 min at 4°C. All FACS experiments were performed on a single BD Aria II machine. Cells were sorted using a 100 μm nozzle in purity mode. Data were analyzed with FlowJo software (Tree Star, San Carlos, CA).

Germ Cell Transplantation

Four independent transplantations were performed. For each transplantation experiment, testes cell suspensions were prepared from two pooled adult mice and sorted as described above. A total of 16–18 recipient testes was analyzed per cell type. Donor cells were introduced into infertile $Kit^{W/Wv}$ recipients (Jackson Laboratory) via efferent duct injection (Ogawa et al., 1997). Colonization was determined 8 weeks after injection. Colony numbers were normalized to 100,000 cells transplanted. Statistics were calculated using Prism (GraphPad Software, La Jolla, CA) using the Mann-Whitney non-parametric U test.

RNA-Seq Library Preparation

Dissociated testes cells were prepared and sorted from both testes of adult mice, as described previously (Pech et al., 2015). Four to five biological replicates were sorted per cell population. cDNA was prepared and amplified using the NuGEN Ovation V2 kit, starting from 5 to 10 ng of total RNA. cDNA was sonicated to 200 bp using a Covaris S2 machine, and 25 ng of cDNA was used to make the libraries, following standard Illumina TruSeq v2 protocols. Samples were sequenced on an Illumina HiSeq 2500 machine, with paired-end 101 bp reads.

ACCESSION NUMBERS

The accession number for the RNA-seq data reported in this paper is GEO: GSE107694.

SUPPLEMENTAL INFORMATION

Supplemental Information includes Supplemental Experimental Procedures, five figures, and three tables and can be found with this article online at https://doi.org/10.1016/j.stemcr.2017.12.009.

AUTHOR CONTRIBUTIONS

A.G. and M.F.P. carried out the majority of the experiments. A.G. performed the bioinformatics analysis. M.F.P. generated the

Tert-Tomato mouse and performed whole mounts. K.H. contributed MCAM cytospin and qPCR data. M.S. performed the transplantation experiments with support from K.E.O. R.J.Z. carried out the mouse husbandry. A.G., M.F.P., and S.E.A. conceived the study, designed the experiments, and wrote the manuscript.

ACKNOWLEDGMENTS

This work was supported by NIH grants CA197563 and AG056575. We thank members of the Artandi lab for critical comments. A.G. was funded by a National Science Foundation National Research Service Award fellowship. M.P. was supported by a National Science Foundation National Research Service Award fellowship and a T32 training grant (CA09302). We acknowledge the Stanford Neuroscience Microscopy Service (NIH grant NS069375) and the Stanford Shared FACS Facility.

Received: July 15, 2017
Revised: December 8, 2017
Accepted: December 11, 2017
Published: January 11, 2018

REFERENCES

Aloisio, G.M., Nakada, Y., Saatcioglu, H.D., Pena, C.G., Baker, M.D., Tarnawa, E.D., Mukherjee, J., Manjunath, H., Bugde, A., Sengupta, A.L., et al. (2014). PAX7 expression defines germline stem cells in the adult testis. J. Clin. Invest. *124*, 3929–3944.

Beumer, T.L., Roepers-Gajadien, H.L., Gademan, I.S., Kal, H.B., and de Rooij, D.G. (2000). Involvement of the D-type cyclins in germ cell proliferation and differentiation in the mouse. Biol. Reprod. *63*, 1893–1898.

Branney, P.A., Faas, L., Steane, S.E., Pownall, M.E., and Isaacs, H.V. (2009). Characterisation of the fibroblast growth factor dependent transcriptome in early development. PLoS One *4*, e4951.

Brinster, R.L., and Zimmermann, J.W. (1994). Spermatogenesis following male germ-cell transplantation. Proc. Natl. Acad. Sci. USA *91*, 11298–11302.

Buageaw, A., Sukhwani, M., Ben-Yehudah, A., Ehmcke, J., Rawe, V.Y., Pholpramool, C., Orwig, K.E., and Schlatt, S. (2005). GDNF family receptor alpha1 phenotype of spermatogonial stem cells in immature mouse testes1. Biol. Reprod. *73*, 1011–1016.

Chakraborty, P., Buaas, F.W., Sharma, M., Snyder, E., de Rooij, D.G., and Braun, R.E. (2014). LIN28A marks the spermatogonial progenitor population and regulates its cyclic expansion. Stem Cells *32*, 860–873.

de Rooij, D.G. (1973). Spermatogonial stem cell renewal in the mouse. I. Normal situation. Cell Tissue Kinet. *6*, 281–287.

Ernst, J., and Bar-Joseph, Z. (2006). STEM: a tool for the analysis of short time series gene expression data. BMC Bioinformatics *7*, 191.

Gassei, K., and Orwig, K.E. (2013). SALL4 expression in gonocytes and spermatogonial clones of postnatal mouse testes. PLoS One *8*, e53976.

Grasso, M., Fuso, A., Dovere, L., de Rooij, D.G., Stefanini, M., Boitani, C., and Vicini, E. (2012). Distribution of GFRA1– expressing spermatogonia in adult mouse testis. Reproduction *143*, 325–332.

Grisanti, L., Falciatori, I., Grasso, M., Dovere, L., Fera, S., Muciaccia, B., Fuso, A., Berno, V., Boitani, C., Stefanini, M., et al. (2009). Identification of spermatogonial stem cell subsets by morphological analysis and prospective isolation. Stem Cells *27*, 3043–3052.

Hara, K., Nakagawa, T., Enomoto, H., Suzuki, M., Yamamoto, M., Simons, B.D., and Yoshida, S. (2014). Mouse spermatogenic stem cells continually interconvert between equipotent singly isolated and syncytial states. Cell Stem Cell *14*, 658–672.

Hasegawa, K., Namekawa, S.H., and Saga, Y. (2013). MEK/ERK signaling directly and indirectly contributes to the cyclical self-renewal of spermatogonial stem cells. Stem Cells *31*, 2517–2527.

Hasegawa, K., and Saga, Y. (2014). FGF8-FGFR1 signaling acts as a niche factor for maintaining undifferentiated spermatogonia in the mouse. Biol. Reprod. *91*, 145.

He, Z., Jiang, J., Kokkinaki, M., Golestaneh, N., Hofmann, M.-C., and Dym, M. (2008). Gdnf upregulates c-Fos transcription via the Ras/Erk1/2 pathway to promote mouse spermatogonial stem cell proliferation. Stem Cells *26*, 266–278.

Helsel, A.R., Yang, Q.-E., Oatley, M.J., Lord, T., Sablitzky, F., and Oatley, J.M. (2017). ID4 levels dictate the stem cell state in mouse spermatogonia. Development *144*, 624–634.

Huckins, C. (1971). The spermatogonial stem cell population in adult rats. I. Their morphology, proliferation and maturation. Anat. Rec. *169*, 533–557.

Ikami, K., Tokue, M., Sugimoto, R., Noda, C., Kobayashi, S., Hara, K., and Yoshida, S. (2015). Hierarchical differentiation competence in response to retinoic acid ensures stem cell maintenance during mouse spermatogenesis. Development *142*, 1582–1592.

Kanatsu-Shinohara, M., Morimoto, H., and Shinohara, T. (2012). Enrichment of mouse spermatogonial stem cells by melanoma cell adhesion molecule expression. Biol. Reprod. *87*, 139.

Kanatsu-Shinohara, M., Ogonuki, N., Inoue, K., Miki, H., Ogura, A., Toyokuni, S., and Shinohara, T. (2003). Long-term proliferation in culture and germline transmission of mouse male germline stem cells. Biol. Reprod. *69*, 612–616.

Kanatsu-Shinohara, M., Takashima, S., Ishii, K., and Shinohara, T. (2011). Dynamic changes in EPCAM expression during spermatogonial stem cell differentiation in the mouse testis. PLoS One *6*, e23663.

Kluin, P.M., Kramer, M.F., and de Rooij, D.G. (1982). Spermatogenesis in the immature mouse proceeds faster than in the adult. Int. J. Androl. *5*, 282–294.

Komai, Y., Tanaka, T., Tokuyama, Y., Yanai, H., Ohe, S., Omachi, T., Atsumi, N., Yoshida, N., Kumano, K., Hisha, H., et al. (2014). Bmi1 expression in long-term germ stem cells. Sci. Rep. *4*, 6175.

Kubota, H., Avarbock, M.R., and Brinster, R.L. (2003). Spermatogonial stem cells share some, but not all, phenotypic and functional characteristics with other stem cells. Proc. Natl. Acad. Sci. USA *100*, 6487–6492.

Lee, H.W., Blasco, M.A., Gottlieb, G.J., Horner, J.W., 2nd, Greider, C.W., and DePinho, R.A. (1998). Essential role of mouse telomerase in highly proliferative organs. Nature *392*, 569–574.

Lee, J., Kanatsu-Shinohara, M., Morimoto, H., Kazuki, Y., Takashima, S., Oshimura, M., Toyokuni, S., and Shinohara, T. (2009). Genetic reconstruction of mouse spermatogonial stem

cell self-renewal in vitro by Ras-cyclin D2 activation. Cell Stem Cell *5*, 76–86.

Meng, X., Lindahl, M., Hyvonen, M.E., Parvinen, M., de Rooij, D.G., Hess, M.W., Raatikainen-Ahokas, A., Sainio, K., Rauvala, H., Lakso, M., et al. (2000). Regulation of cell fate decision of undifferentiated spermatogonia by GDNF. Science *287*, 1489–1493.

Merico, D., Isserlin, R., Stueker, O., Emili, A., and Bader, G.D. (2010). Enrichment map: a network-based method for gene-set enrichment visualization and interpretation. PLoS One *5*, e13984.

Nakagawa, T., Nabeshima, Y., and Yoshida, S. (2007). Functional identification of the actual and potential stem cell compartments in mouse spermatogenesis. Dev. Cell *12*, 195–206.

Nakagawa, T., Sharma, M., Nabeshima, Y.i., Braun, R.E., and Yoshida, S. (2010). Functional hierarchy and reversibility within the murine spermatogenic stem cell compartment. Science *328*, 62–67.

Oakberg, E.F. (1971). Spermatogonial stem-cell renewal in the mouse. Anat. Rec. *169*, 515–531.

Oatley, J.M., Avarbock, M.R., Telaranta, A.I., Fearon, D.T., and Brinster, R.L. (2006). Identifying genes important for spermatogonial stem cell self-renewal and survival. Proc. Natl. Acad. Sci. USA *103*, 9524–9529.

Ogawa, T., Arechaga, J.M., Avarbock, M.R., and Brinster, R.L. (1997). Transplantation of testis germinal cells into mouse seminiferous tubules. Int. J. Dev. Biol. *41*, 111–122.

Pech, M.F., Garbuzov, A., Hasegawa, K., Sukhwani, M., Zhang, R.J., Benayoun, B.A., Brockman, S.A., Lin, S., Brunet, A., Orwig, K.E., et al. (2015). High telomerase is a hallmark of undifferentiated spermatogonia and is required for maintenance of male germline stem cells. Genes Dev. *29*, 2420–2434.

Phillips, B.T., Gassei, K., and Orwig, K.E. (2010). Spermatogonial stem cell regulation and spermatogenesis. Philos. Trans. R. Soc. Lond. B Biol. Sci. *365*, 1663–1678.

Schrans-Stassen, B.H., van de Kant, H.J., de Rooij, D.G., and van Pelt, A.M. (1999). Differential expression of c-kit in mouse undifferentiated and differentiating type A spermatogonia. Endocrinology *140*, 5894–5900.

Shinohara, T., Avarbock, M.R., and Brinster, R.L. (1999). beta1– and alpha6-integrin are surface markers on mouse spermatogonial stem cells. Proc. Natl. Acad. Sci. USA *96*, 5504–5509.

Spradling, A., Fuller, M.T., Braun, R.E., and Yoshida, S. (2011). Germline stem cells. Cold Spring Harb. Perspect. Biol. *3*, a002642.

Suzuki, H., Ahn, H.W., Chu, T., Bowden, W., Gassei, K., Orwig, K., and Rajkovic, A. (2012). SOHLH1 and SOHLH2 coordinate spermatogonial differentiation. Dev. Biol. *361*, 301–312.

Suzuki, H., Sada, A., Yoshida, S., and Saga, Y. (2009). The heterogeneity of spermatogonia is revealed by their topology and expression of marker proteins including the germ cell-specific proteins Nanos2 and Nanos3. Dev. Biol. *336*, 222–231.

Tadokoro, Y., Yomogida, K., Ohta, H., Tohda, A., and Nishimune, Y. (2002). Homeostatic regulation of germinal stem cell proliferation by the GDNF/FSH pathway. Mech. Dev. *113*, 29–39.

Tokuda, M., Kadokawa, Y., Kurahashi, H., and Marunouchi, T. (2007). CDH1 is a specific marker for undifferentiated spermatogonia in mouse testes1. Biol. Reprod. *76*, 130–141.

van Haaster, L.H., and de Rooij, D.G. (1993). Spermatogenesis is accelerated in the immature Djungarian and Chinese hamster and rat. Biol. Reprod. *49*, 1229–1235.

Stem Cell Reports, Volume *10*

Supplemental Information

Purification of GFRα1+ and GFRα1– Spermatogonial Stem Cells Reveals a Niche-Dependent Mechanism for Fate Determination

Alina Garbuzov, Matthew F. Pech, Kazuteru Hasegawa, Meena Sukhwani, Ruixuan J. Zhang, Kyle E. Orwig, and Steven E. Artandi

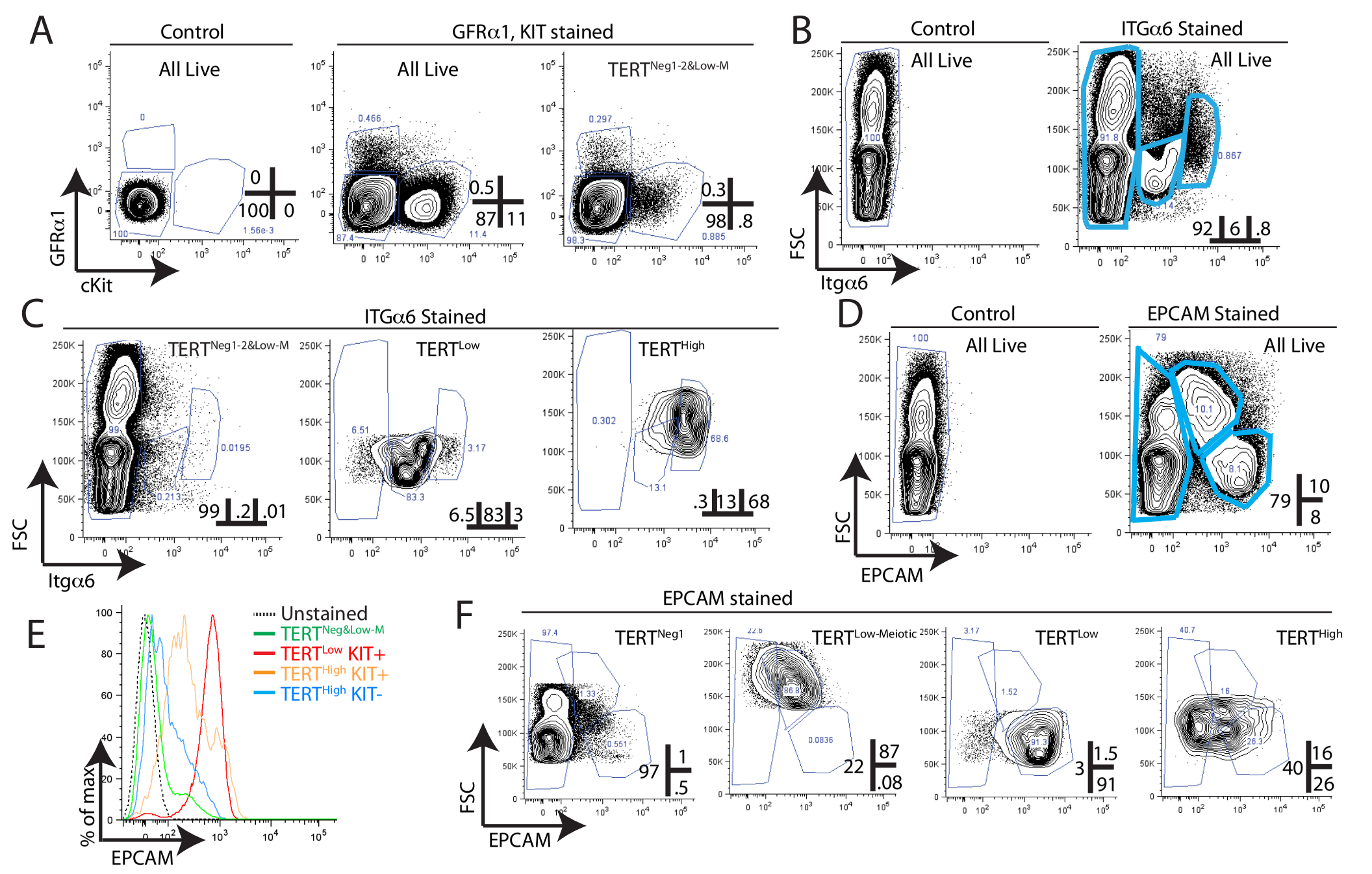

G

Cell Type	Tert-Tomato	Itga6	EPCAM	KIT	THY1	GFRa1
A-undiff	++++	+++	-/+	-	+or -	+or -
Early A-diff	+++	++	-/+	++	-	-
Late A-diff	++	+	+++	+	-	-
Meiosis I	+	-	++	-	-	-
Spermatids	-	-	-	-	-	-

Fig. S1

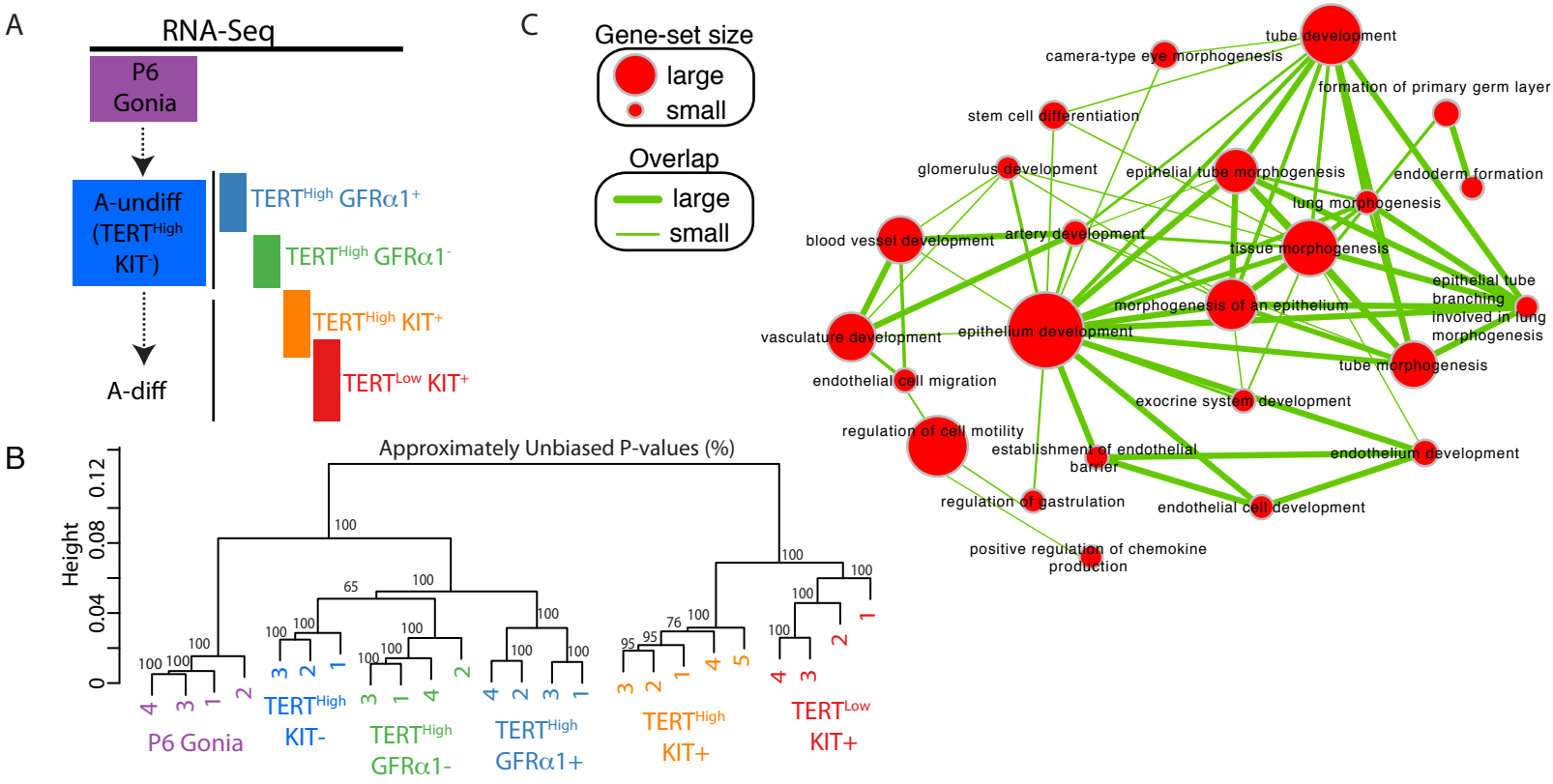
A
RNA-Seq
P6 Gonia
A-undiff (TERTHigh KIT-)
A-diff
TERTHigh GFRα1+
TERTHigh GFRα1-
TERTHigh KIT+
TERTLow KIT+
B
Approximately Unbiased P-values (%)
Height
0
0.04
0.08
0.12
P6 Gonia
TERTHigh KIT-
TERTHigh GFRα1-
TERTHigh GFRα1+
TERTHigh KIT+
TERTLow KIT+
C
Gene-set size
large
small
Overlap
large
small
tube development
camera-type eye morphogenesis
formation of primary germ layer
stem cell differentiation
glomerulus development
epithelial tube morphogenesis
endoderm formation
lung morphogenesis
blood vessel development
artery development
tissue morphogenesis
epithelial tube branching involved in lung morphogenesis
morphogenesis of an epithelium
vasculature development
epithelium development
tube morphogenesis
endothelial cell migration
exocrine system development
regulation of cell motility
establishment of endothelial barrier
endothelium development
regulation of gastrulation
endothelial cell development
positive regulation of chemokine production

Fig. S2

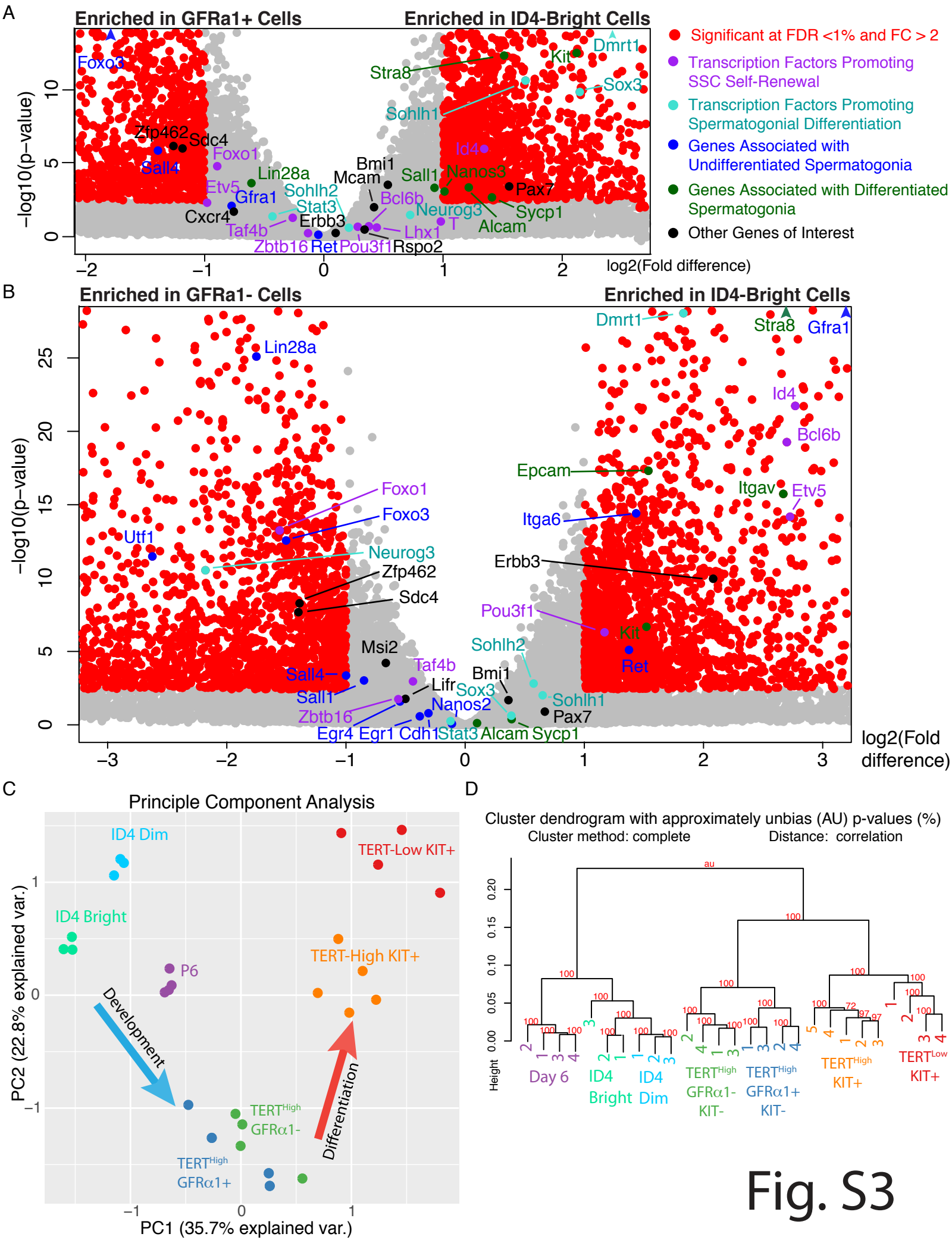
A
Enriched in GFRa1+ Cells
Enriched in ID4-Bright Cells
−log10(p−value)
log2(Fold difference)
Foxo3
Zfp462
Sdc4
Sall4
Foxo1
Etv5
Gfra1
Lin28a
Cxcr4
Sohlh2
Stat3
Taf4b
Erbb3
Zbtb16
Ret
Bmi1
Mcam
Pou3f1
Rspo2
Bcl6b
Lhx1
Sall1
Id4
Nanos3
Neurog3
T
Alcam
Pax7
Sycp1
Stra8
Kit
Dmrt1
Sox3
Sohlh1
Significant at FDR <1% and FC > 2
Transcription Factors Promoting SSC Self-Renewal
Transcription Factors Promoting Spermatogonial Differentiation
Genes Associated with Undifferentiated Spermatogonia
Genes Associated with Differentiated Spermatogonia
Other Genes of Interest
B
Enriched in GFRa1- Cells
Enriched in ID4-Bright Cells
−log10(p−value)
log2(Fold difference)
Lin28a
Foxo1
Foxo3
Utf1
Neurog3
Zfp462
Sdc4
Msi2
Sall4
Taf4b
Lifr
Sall1
Zbtb16
Egr4
Egr1
Cdh1
Nanos2
Stat3
Bmi1
Sox3
Alcam
Pax7
Sohlh1
Sycp1
Pou3f1
Sohlh2
Kit
Ret
Erbb3
Epcam
Itga6
Itgav
Etv5
Id4
Bcl6b
Dmrt1
Stra8
Gfra1
C
Principle Component Analysis
PC2 (22.8% explained var.)
PC1 (35.7% explained var.)
ID4 Dim
ID4 Bright
P6
TERT-Low KIT+
TERT-High KIT+
TERTHigh GFRα1-
TERTHigh GFRα1+
Development
Differentiation
D
Cluster dendrogram with approximately unbias (AU) p-values (%)
Cluster method: complete
Distance: correlation
Height
Day 6
ID4 Bright
ID4 Dim
TERTHigh GFRα1- KIT-
TERTHigh GFRα1+ KIT-
TERTHigh KIT+
TERTLow KIT+

Fig. S3

A

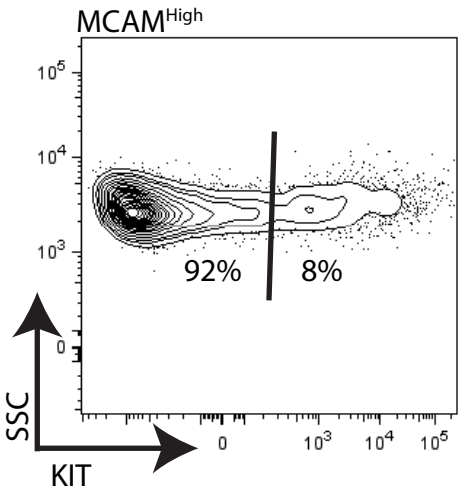
MCAM^High
92%
8%
SSC
KIT

B

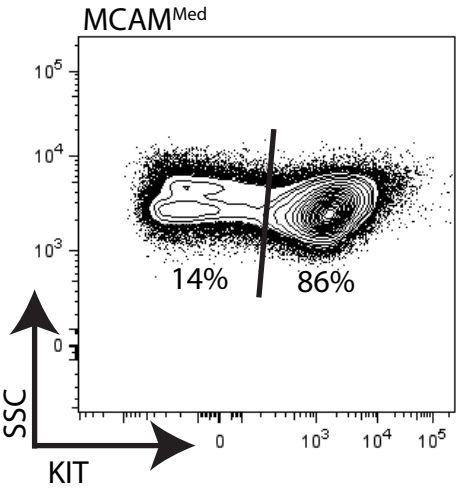
MCAM^Med
14%
86%
SSC
KIT

C

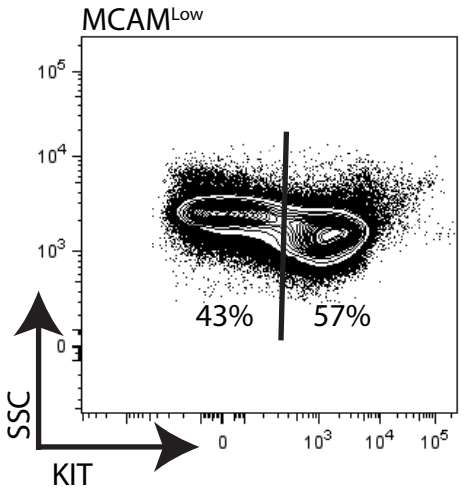
MCAM^Low
43%
57%
SSC
KIT

Fig. S4

A

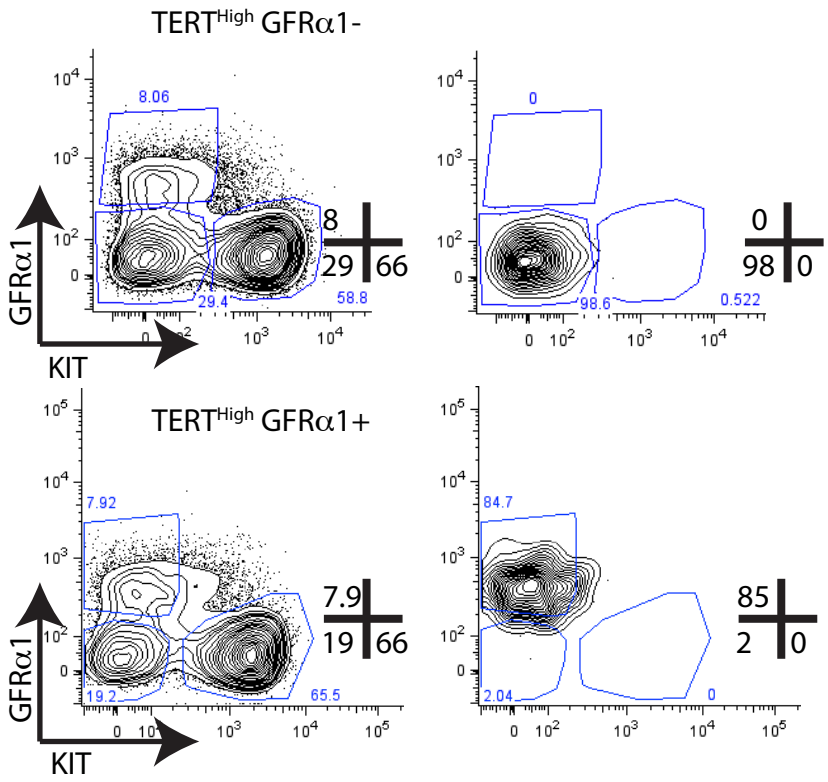
TERT^High GFRα1-
8.06
8
29
66
29.4
58.8
0
0
98
0
98.6
0.522
GFRα1
KIT
TERT^High GFRα1+
7.92
7.9
19
66
19.2
65.5
84.7
85
2
0
2.04
0
GFRα1
KIT

B

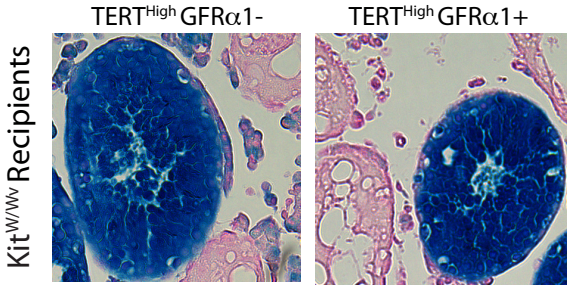
TERT^High GFRα1-
TERT^High GFRα1+
Kit^W/Wv Recipients

Fig. S5

Supplemental Figure Legends

Figure S1. Additional immunophenotyping of adult Tert$^{Tomato/+}$ testis cells, related to Figure 1.

A. Live singlet Tert-Tomato testes cells stained with GFRα1-biotin, streptavidin-APC and cKit antibodies. Control cells are stained with streptavidin-APC only. Background staining of GFRα1 and cKit in meiotic cells is also shown.

B. Live singlet Tert-Tomato testes cells stained with α6-integrin (ITGα6) antibodies. Control cells are unstained.

C. ITGα6 expression in Tert$^{Neg1\text{-}2+Low\text{-}meiotic}$, Tert^{Low} and Tert^{High} cells, graphed against forward-scatter.

D. Live singlet Tert-Tomato testes cells stained with EPCAM antibodies. Control cells are unstained.

E. Histogram of EPCAM expression in the indicated cell populations

F. EPCAM expression in Tert^{Neg1}, Tert$^{Low\text{-}Meioic}$, Tert^{Low} and Tert^{High} cells, graphed against forward-scatter.

G. Summary of immunophenotyping the adult testis. "-" indicates absence of staining. "+" indicates relative degree of staining intensity. "+ or -" indicates bimodal staining pattern.

Figure S2. Clustering of RNA-Seq libraries from biological replicates, related to Figure 2

A. Indicated purified populations were sequenced and the resulting expression data was analyzed using the pvClust package.

B. Shown tree is a result of unsupervised hierarchical clustering using pvClust.

C. Morphogenesis/epithelial development cluster generated by Cytoscape Enrichment Map of GSEA results for Tert^{High} GFRα1+.

Figure S3. Comparison of ID4 RNA-Seq to our sequencing of GFRα1+ and GFRα1- spermatogonia, related to Figure 2.

A. Volcano plot showing differentially expressed genes between GFRα1+ and ID4-Bright cells.

B. Volcano plot showing differentially expressed genes between GFRα1- and ID4-Bright cells.

C. PCA analysis showing relatedness between ID-Bright and ID-Dim cells and our five populations.

D. Unsupervised hierarchical clustering using pvClust of ID-Bright and ID-Dim and our five indicated populations.

Figure S4. cKit Expression in MCAM fractions, related to Figure 4

A. Percent of cKit+ and cKit- cells in the MCAM-High population by flow cytometry.

B. Percent of cKit+ and cKit- cells in the MCAM-Med population by flow cytometry.

C. Percent of cKit+ and cKit- cells in the MCAM-Low population by flow cytometry.

Figure S5. Purity and MCAM status of transplanted GFRα1- cells, related to Figure 5.

A. Representative purity of FACS-sorted cells used for transplantation experiments. Initial gating strategy is shown in the left panel; in the right panel, an aliquot of 500-1000 sorted cells was re-analyzed to determine purity levels

B. Representative histological cross-sections from transplant recipients. R26-lacZ^{+} donor cells of the indicated immunophenotype were labeled by X-gal staining.

Supplemental Experimental Procedures

Wholemount analysis of seminiferous tubules

Wholemount analysis was performed as previously described (Pech et al., 2015). For MCAM wholemounts, the NP40 and methanol treatments were replaced by treatment with -20C acetone for 10min. For wholemounts of GFRα1 expression in the post-transplant testis, no permeabilization steps were used.

Immunofluorescence of FACS-sorted cells

Cytospins and microscopy for Edu, PLZF, and GFRα1 were performed as previously described (Pech et al., 2015). Statistical analysis of Edu incorporation was done using the paired two-tailed Student's t-test. N=5 mice; N=900-10,000 cells per condition. For PLZF and GFRα1 staining, N=3 mice pooled; N=1524 cells were used.

In situ hybridization for Ngn3

In situ hybridization was performed using the RNAScope 2.0 HD reagent Red Kit (Advanced Cell Diagnostics) with a Ngn3 probe (ACD; cat no. 422401) according to the manufacturer's protocol on sorted cells cytospin onto coverslips. Statistical analysis of Ngn3 expression was done using the paired two-tailed Student's t-test. N=5-6 mice; at least N=2000 cells counted per condition.

In vitro germ cell culture

Germ cells were cultured as previously described (Kanatsu-Shinohara et al., 2003a), with minor modifications. Germ cells were sorted using a flow cytometer directly into "basal GS media" (StemPro34 Serum Free Media (Invitrogen), and appropriate supplements. Sorted cells were then transferred to 24-well plates containing irradiated MEF-coated coverslips. Cells were cultured in 2mls of the basal GS media, or basal GS media supplemented with 10ng/ml FGF2 and 50ng/ml GDNF (Peprotech). Immunofluorescence was performed as described above. Statistical analysis of MCAM expression was performed using the unpaired two-tailed Student's t-test. For the experiment, N=4 mice; N=50 cells per condition were used.

RNA-Seq library preparation

Dissociated testes cells were prepared and sorted from both testes of adult mice, as described previously (Pech et al., 2015). Four to five biological replicates were sorted. Cells were sorted directly into Trizol LS (Invitrogen), and RNA extracted following the manufacturer's recommendation. RNA was further purified on Rneasy Micro columns (Qiagen). cDNA was prepared and amplified using the Nugen Ovation V2 kit, starting from 5 to 10ng of total RNA. The cDNA was sonicated to 200bp size using a Covaris S2 machine, and 25ng of cDNA was used to make the libraries, following standard Illumina Truseq V2 protocols. Samples were sequenced on an Illumina Hiseq2500 machine, with paired-end 101bp reads.

Germ Cell Transplantation

Four independent transplantations were performed. For each transplantation experiment, testes cell suspensions were prepared from two pooled adult mice and sorted as described previously. A total of 16-18 recipient testes were analyzed per cell type. Donor cells were genetically marked using either a R26-lacZ allele (Jackson Labs), or a ubiquitously expressed CAG-EGFP allele (Lin and Artandi, unpublished). Cells were sorted in HBSS+5%FBS. Sort purity was confirmed by re-analysis post-sort. Cell yields were confirmed post-sort by hemocytometer. Donor cells were introduced into infertile Kit^{W/W^v} recipients (Jackson Labs) via efferent duct injection (Ogawa et al., 1997). Colonization was determined eight weeks after injection, either by X-gal staining or by EGFP epifluorescence. Colony numbers were normalized to 100,000 cells transplanted. Statistics were calculated using Prism (GraphPad Software, La Jolla, CA) using the Mann-Whitney non-parametric U test.

RNA-Seq data analysis

Differential expression analysis was performed as previously described (Pech et al., 2015). Expression datasets were ordered from the least to most differentiated and submitted with four replicates each to STEM software analysis (Short Time Series Expression Mining, Version 1.0) (Ernst and Bar-Joseph, 2006) using the default parameter setting. Gene Set Enrichment Analysis (GSEA) (Subramanian et al., 2005) was performed using version 2.0.13. Genes were rank-ordered by their T-test value. Genes that could not be converted to a HUGO gene name were excluded. GSEA was run on this pre-ranked list of genes, using default parameters. Results from GSEA were submitted to Cytoscape 3.4 using the Enrichment Map plugin (Merico et al., 2010) using a p-value cutoff of 0.001, a q-value cutoff of 0.05, and a similarity cutoff of 0.5.